Geophys. J. Int. (1995) **123**, 449–470

A new method for computing highly accurate DSM synthetic seismograms

Robert J. Geller and Nozomu Takeuchi

Department of Earth and Planetary Physics, Faculty of Science, Tokyo University, Yayoi 2-11-16, *Bunkyo-ku, Tokyo* 113, *Japan*

Accepted 1995 May 17. Received 1995 May 10; in original form 1995 March 5.

SUMMARY

We derive modified matrix operators that minimize the numerical error of solutions of the discretized elastic equation of motion. The criterion for obtaining the modified matrix operators is that the net error of the discretized equation of motion must be approximately equal to zero whenever the operand is an eigenfunction and the frequency is equal to the corresponding eigenfrequency. As it is not necessary to know the explicit values of the eigensolutions, our approach can be applied to arbitrarily heterogeneous media. In this paper we primarily consider frequency domain solutions calculated using the direct solution method (DSM) (Geller *et al.* 1990; Hara, Tsuboi & Geller 1991; Geller & Ohminato 1994). We present explicit formulations of the modified operators and numerical examples for *P-SV* and *SH* wave propagation in laterally homogeneous, isotropic media. The numerical solutions obtained using the modified operators are about 30 times more accurate than those obtained using the unmodified operators for the same CPU time. Our methods are readily applicable to problems in spherical coordinates or involving laterally heterogeneous media, as well as to time-domain solutions. It should also be possible to apply the methods of this paper to numerical methods other than the DSM.

Key words: direct solution method (DSM), numerical error, synthetic seismograms.

1 INTRODUCTION

Great progress in determining 3-D Earth structure was made in the 1970s and 1980s by analysing body-wave traveltimes and surface-wave phase velocities. It now seems to be the general consensus that such studies have reached the point of diminishing returns, and that further progress can only be made by inversion of seismic waveforms themselves, rather than secondary parameters such as traveltimes or phase velocities (e.g. Nolet, Grand & Kennett 1994).

Techniques for inverting seismic waveform data for Earth structure (e.g. Tarantola 1984; Geller & Hara 1993) require highly accurate synthetic seismograms to obtain accurate earth models. Synthetics for use in waveform inversion studies must therefore meet a much stricter standard of accuracy than has heretofore been thought necessary for forward modelling. The purpose of this paper is to derive and implement numerical methods that optimize the accuracy of the synthetic seismograms for a given CPU time, i.e. for a given grid spacing and matrix bandwidth. This paper considers calculations for laterally homogeneous media with Cartesian or cylindrical coordinates. However, numerical methods of the type presented in this paper can also be readily applied to problems in spherical coordinates. Cummins *et al.* (1994a) have already presented modified operators for toroidal (*SH*) synthetics, and the methods of Cummins, Geller & Takeuchi (1994b) for spheroidal (*P-SV*) synthetics for a laterally homogeneous spherical model can be readily adapted to use the modified operators presented in this paper. Our methods should also be applicable to the laterally heterogeneous spherical case considered by Cummins, Geller & Takeuchi (1994c).

Hybrid approaches are also possible. Geller & Hatori (1995) presented a DSM formulation for a plane-layered medium using analytic trial functions. It is straightforward to use their analytical trial functions for the plane-layered part of the medium, and the numerical methods of this paper for the part of the medium with continuous velocity gradients. The two formulations can be joined by simply 'overlapping' the mass and stiffness matrices at the boundary.

1.1 Preview

We consider a homogeneous region in this subsection, although the derivations below consider inhomogeneous media. We assume that separation of variables has already been used to reduce the problem to a system of coupled ordinary differential equations with z as the independent variable.

As is well known, discretized operators have errors due to numerical dispersion. For example, the three-point finite-difference operator for a second derivative yields

$$\frac{1}{\Delta z^2}[u(z-\Delta z)-2u(z)+u(z+\Delta z)]=\frac{d^2u}{dz^2}+\frac{\Delta z^2}{12}\frac{d^4u}{dz^4}+\cdots, \tag{1.1}$$

rather than the desired value

$$\frac{d^2u}{dz^2}. \tag{1.2}$$

The second term in eq. (1.1) is the error due to numerical dispersion. The Taylor series expansions used to derive eq. (1.1) and later results in this section are given below in eqs (3.20)–(3.23).

In the next section, we derive a general criterion for optimally accurate modified operators: the net error of the discretized equation of motion should be approximately equal to zero when the operand is an eigenfunction and the frequency is equal to the corresponding eigenfrequency. To satisfy this criterion, we define modified operators for the first- and zeroth-derivative operators whose leading error term matches that of the second-derivative operator in eq. (1.1).

The commonly used three-point operator for the first derivative is

$$\frac{1}{2\Delta z}[u(z+\Delta z)-u(z-\Delta z)]=\frac{du}{dz}+\frac{\Delta z^2}{6}\frac{d^3u}{dz^3}+\cdots. \tag{1.3}$$

However, to match the leading error term in eq. (1.1), the coefficient of the leading error term of the discretized operator for the first derivative must be $\Delta z^2/12$ rather than the factor of $\Delta z^2/6$ in eq. (1.3). We define four-point modified first-derivative operators below that have the desired numerical error.

For the laterally homogeneous cases considered in this paper, the numerical operators for the first derivative occur in the *P-SV* problem, but not in the *SH* problem. The sites occupied by the unmodified first-derivative operators in the matrix of coefficients for the discretized equation of motion are shown by the solid circles and triangles in Fig. 4 (p. 463). However, as shown in Fig. 4, we can also use the sites indicated by the plus signs (odd-numbered rows) or crosses (even-numbered rows) to formulate four-point operators for the first derivative that do not increase the bandwidth of the coefficient matrix. The four-point first-derivative operators for the odd-numbered rows use one extra point to the left,

$$\frac{1}{12\Delta z}[5u(z+\Delta z)+3u(z)-9u(z-\Delta z)+u(z-2\Delta z)]=\frac{du}{dz}+\frac{\Delta z^2}{12}\frac{d^3u}{dz^3}+\cdots, \tag{1.4}$$

while the four-point operators for the even-numbered rows use one extra point to the right,

$$\frac{1}{12\Delta z}[-u(z+2\Delta z)+9u(z+\Delta z)-3u(z)-5u(z-\Delta z)]=\frac{du}{dz}+\frac{\Delta z^2}{12}\frac{d^3u}{dz^3}+\cdots. \tag{1.5}$$

The following 'zeroth-derivative' operator matches the error in eq. (1.1):

$$\tfrac{1}{12}u(z-\Delta z)+\tfrac{5}{6}u(z)+\tfrac{1}{12}u(z+\Delta z)=u+\frac{\Delta z^2}{12}\frac{d^2u}{dz^2}+\cdots. \tag{1.6}$$

The combined use of operators of the form of eqs (1.1), (1.4), (1.5) and (1.6) leads to discretized equations that satisfy the criterion for optimally accurate operators. We have

$$[\text{Discretized equation}(\omega,\mathbf{u})]=[\text{exact equation}(\omega,\mathbf{u})]+\frac{\Delta z^2}{12}[\text{exact equation}(\omega,\mathbf{u})]''+\cdots, \tag{1.7}$$

where the prime denotes differentiation with respect to z. Now suppose $\mathbf{u}_m$ is the eigenfunction of a mode and ω_m is the corresponding eigenfrequency. In this case,

$$[\text{exact equation}(\omega_m,\mathbf{u}_m)]=0, \tag{1.8}$$

and therefore

$$[\text{exact equation}(\omega_m,\mathbf{u}_m)]''=[0]''=0. \tag{1.9}$$

Substituting eqs (1.8) and (1.9) into eq. (1.7), we obtain

$$[\text{Discretized equation}(\omega_m,\mathbf{u}_m)]\approx 0. \tag{1.10}$$

As shown in Fig. 4, the full bandwidth for the various operators is not available at the boundaries. Discretized operators with less than the full bandwidth have relatively large 'point-source' errors at the boundaries. However, as we show rigorously in the next section, such point-source operator errors have only a small effect on the error of the solution of the discretized equation. This result is extremely important in designing modified operators. Fig. 8 (p. 469) shows a numerical example confirming this result.

1.2 Relation to previous work

Many papers have studied the numerical dispersion associated with various discretized operators. Marfurt (1984) made phenomenological attempts to improve the accuracy of finite-element solutions of the acoustic and elastic wave equation by replacing the 'consistent mass matrix' by linear combinations of the 'consistent' and 'lumped' mass matrices. Korn (1987) rigorously derived a modified operator for the *SH* (toroidal) problem by finding a form that eliminates numerical dispersion, but could not extend his derivations to other cases. The modified operators derived by Korn for the *SH* case are essentially the same as those derived for the *SH* case in the present paper.

In contrast to these studies, we use the first-order Born approximation to obtain formal expressions for the relative error of the numerical solutions; we then derive operators that minimize the relative error. There are several significant advantages to this approach. First, it is easier to obtain modified operators, especially for the *P-SV* case. Second, we can design operators that correctly handle external and internal boundaries. Third, we can derive modified operators that accurately handle media with velocity gradients. Fourth, we obtain error estimates that allow the grid spacing to be chosen to yield a desired level of accuracy.

2 THEORY

The DSM is a Galerkin weak form method (Strang & Fix 1973) for solving the elastic equation of motion. Detailed derivations are given by Geller & Ohminato (1994) and will not be repeated here. The DSM equation of motion for a medium with free surface boundary conditions is

$$(\omega^2\mathbf{T}-\mathbf{H})\mathbf{c}=-\mathbf{g}, \tag{2.1}$$

where ω is the frequency, $\mathbf{T}$ is the mass (kinetic energy) matrix, $\mathbf{H}$ is the stiffness (potential energy) matrix, $\mathbf{c}$ is the vector of expansion coefficients for the trial functions, and $\mathbf{g}$ is the force vector. In the basis of trial functions, the matrix and vector elements are as follows:

$$T_{mn}=\int_V [\phi_i^{(m)}]^* \rho \phi_i^{(n)}\, dV, \tag{2.2}$$

$$H_{mn}=\int_V [\phi_{i,j}^{(m)}]^* C_{ijkl}\phi_{k,l}^{(n)}\, dV, \tag{2.3}$$

$$g_m=\int_V [\phi_i^{(m)}]^* f_i\, dV, \tag{2.4}$$

where $\phi_i^{(m)}$ is the i-component of the mth trial function, '$,j$' denotes spatial differentiation with respect to the j-coordinate, ρ is the density, C_{ijkl} is the elastic modulus, f_i is the external body force, and '*' denotes complex conjugation. The summation convention applies to subscripts corresponding to physical (x, y or z) coordinates, but not to indices corresponding to abstract vector spaces, such as those denoting trial functions. The displacement is represented as a linear combination of the trial functions,

$$u_i=\sum_n c_n\phi_i^{(n)}. \tag{2.5}$$

The operators defined in eqs (2.2) and (2.3) will not in general be exact. We formally denote the exact operators by $\mathbf{T}^{(0)}$ and $\mathbf{H}^{(0)}$, the exact solution by $\mathbf{c}^{(0)}$, the error of the numerical operators by $\delta\mathbf{T}$ and $\delta\mathbf{H}$, and the error of the numerical solution by $\delta\mathbf{c}$, where

$$\mathbf{T}=\mathbf{T}^{(0)}+\delta\mathbf{T}, \tag{2.6}$$

$$\mathbf{H}=\mathbf{H}^{(0)}+\delta\mathbf{H}, \tag{2.7}$$

$$\mathbf{c}=\mathbf{c}^{(0)}+\delta\mathbf{c}, \tag{2.8}$$

We represent the exact solution, the numerical solution and the error of the numerical solution by eigenfunction expressions from here through to eq. (2.21). It is not necessary to know the actual numerical values of the eigenvalues and eigenvectors.

The normal modes satisfy

$$[\omega_m^2\mathbf{T}^{(0)}-\mathbf{H}^{(0)}]\mathbf{c}_m=0, \tag{2.9}$$

where ω_m is the eigenfrequency of the mth mode, and $\mathbf{c}_m$ is the eigenvector. We assume that the modes are orthonormalized, so that

$$\mathbf{c}_m^*\mathbf{H}^{(0)}\mathbf{c}_n=\omega_m^2\mathbf{c}_m^*\mathbf{T}^{(0)}\mathbf{c}_n=\omega_m^2\delta_{mn}, \tag{2.10}$$

where δ_{mn} is a Kronecker delta.

We assume that anelastic attenuation is included in the elastic moduli. In some cases the eigenvectors for the anelastic case are not orthogonal and $\mathbf{c}_m^*$ must be replaced by the dual space (left) eigenvector (e.g. Park & Gilbert 1986). If necessary, the following derivation can be modified in a straightforward way to takes this into account.

The exact equation of motion can be formally written as follows:

$$[\omega^2\mathbf{T}^{(0)}-\mathbf{H}^{(0)}]\mathbf{c}^{(0)}=-\mathbf{g}. \tag{2.11}$$

The error of the solutions, $\delta\mathbf{c}$, can be estimated using the first-order Born approximation:

$$[\omega^2\mathbf{T}^{(0)} - \mathbf{H}^{(0)}]\delta\mathbf{c} = -(\omega^2\delta\mathbf{T} - \delta\mathbf{H})\mathbf{c}^{(0)}. \tag{2.12}$$

We represent the solution of eq. (2.11) in terms of an eigenfunction expansion,

$$\mathbf{c}^{(0)} = \sum_m d_m^{(0)}\mathbf{c}_m. \tag{2.13}$$

The expansion coefficient of the mth mode is given by

$$d_m^{(0)} = -g_m/(\omega^2 - \omega_m^2), \tag{2.14}$$

where

$$g_m = \mathbf{c}_m^*\mathbf{g}. \tag{2.15}$$

The denominator of the right-hand side (rhs) of eq. (2.14) will be small, and thus $d_m^{(0)}$ will be large, when ω is close to ω_m. $d_m^{(0)}$ will be negligible except when ω is in the vicinity of ω_m.

We also represent the solution of eq. (2.12) in terms of an eigenfunction expansion,

$$\delta\mathbf{c} = \sum_m \delta d_m\mathbf{c}_m. \tag{2.16}$$

The expansion coefficient for the mth mode is given by

$$\delta d_m = -\frac{\sum_n (\omega^2\delta T_{mn} - \delta H_{mn})d_n^{(0)}}{(\omega^2 - \omega_m^2)}. \tag{2.17}$$

By the same argument used above for eq. (2.14), the m-component of the error (i.e. δd_m) will be large only when ω is close to ω_m. However, in the vicinity of $\omega = \omega_m$, only $d_m^{(0)}$ will be large; the expansion coefficients of all the other modes will be negligible. Therefore in the vicinity of $\omega = \omega_m$, the $n \neq m$ terms in the summation in eq. (2.17) can be neglected. The expansion coefficient of the mth mode for the numerical error is therefore approximately given by

$$\delta d_m = -\frac{(\omega^2\delta T_{mm} - \delta H_{mm})d_m^{(0)}}{(\omega^2 - \omega_m^2)}. \tag{2.18}$$

We thus see from eq. (2.18) that the relative error of the numerical solution in the vicinity of $\omega = \omega_m$ can be approximated by

$$\frac{\delta d_m}{d_m^{(0)}} = -\frac{(\omega^2\delta T_{mm} - \delta H_{mm})}{(\omega^2 - \omega_m^2)} = -\frac{\delta T_{mm}(\omega^2 - \delta H_{mm}/\delta T_{mm})}{(\omega^2 - \omega_m^2)}. \tag{2.19}$$

Note that in the cases of interest ω will be real, but ω_m will include a small imaginary part due to anelastic attenuation. Therefore, the denominators in eqs (2.14), (2.17), (2.18) and (2.19) will become small as $\omega \to \omega_m$, but will never exactly equal zero.

Eq. (2.19) shows that in general the relative error will greatly increase as ω approaches ω_m. However, if the numerator of eq. (2.19) is also proportional to $(\omega^2 - \omega_m^2)$, the relative error will not worsen appreciably as $\omega \to \omega_m$. Such proportionality can be achieved if and only if the errors of the numerical operators approximately satisfy

$$\omega_m^2\delta T_{mm} - \delta H_{mm} = 0 \tag{2.20}$$

for every mode. Eq. (2.20) implies that the matrix elements for coupling between modes, δT_{mn} and δH_{mn}, $m \neq n$, do not significantly affect the error of the numerical solution.

Eq. (2.19) shows that the relative error of the numerical solution obtained using modified operators that approximately satisfy eq. (2.20) is approximately given by

$$\left|\frac{\delta d_m}{d_m^{(0)}}\right| = |\delta T_{mm}|, \tag{2.21}$$

even as $\omega \to \omega_m$. On the other hand, if the operators do not approximately satisfy eq. (2.20), then eq. (2.19) shows that the relative error will worsen drastically as $\omega \to \omega_m$.

The original DSM operators will not in general satisfy eq. (2.20). In this paper we derive modified operators $\mathbf{T}'$ and $\mathbf{H}'$ which have the same bandwidth as $\mathbf{T}$ and $\mathbf{H}$ but which approximately satisfy eq. (2.20) to the lowest relevant order of Δz, where Δz is the grid spacing.

The matrix elements in eq. (2.20) are given in any basis by

$$\begin{aligned} T_{mn} &= \mathbf{c}_m^*\mathbf{T}\mathbf{c}_n, & T'_{mn} &= \mathbf{c}_m^*\mathbf{T}'\mathbf{c}_n, \\ H_{mn} &= \mathbf{c}_m^*\mathbf{H}\mathbf{c}_n, & H'_{mn} &= \mathbf{c}_m^*\mathbf{H}'\mathbf{c}_n, \\ \delta T_{mn} &= \mathbf{c}_m^*\delta\mathbf{T}\mathbf{c}_n, & \delta T'_{mn} &= \mathbf{c}_m^*\delta\mathbf{T}'\mathbf{c}_n, \\ \delta H_{mn} &= \mathbf{c}_m^*\delta\mathbf{H}\mathbf{c}_n, & \delta H'_{mn} &= \mathbf{c}_m^*\delta\mathbf{H}'\mathbf{c}_n. \end{aligned} \tag{2.22}$$

Using eqs (2.20) and (2.22), we see that in any basis the error of the modified operators must approximately satisfy

$$\mathbf{c}_m^*(\omega_m^2\delta\mathbf{T}' - \delta\mathbf{H}')\mathbf{c}_m = 0. \tag{2.23}$$

Using eqs (2.6), (2.7), and (2.9), we see that eq. (2.23) is equivalent to

$$\mathbf{c}_m^*(\omega_m^2\mathbf{T}' - \mathbf{H}')\mathbf{c}_m = 0. \tag{2.24}$$

2.1 Physical interpretation

In this subsection only, we use $\omega_m^{(0)}$ and $\mathbf{c}_m^{(0)}$ to denote the eigenfrequencies and eigenvectors of the exact operators. The eigenfrequencies, ω_m^2, and eigenvectors, $\mathbf{c}_m$, of the original numerical operators $\mathbf{T}$ and $\mathbf{H}$ are solutions of

$$(\omega_m^2\mathbf{T} - \mathbf{H})\mathbf{c}_m = 0. \tag{2.25}$$

By comparing eq. (2.25) with eq. (2.9), and using eqs (2.6) and (2.7), we can find the relation between the exact eigenfrequencies, $\omega_m^{(0)}$, and the eigenfrequencies of the numerical operators ω_m. If we define $\delta\omega_m = \omega_m - \omega_m^{(0)}$, then, using standard results from first-order perturbation theory, the error of the eigenfrequencies of the original operators is found to be

$$2\omega_m^{(0)}\delta\omega_m = \delta H_{mm} - \omega_m^{(0)^2}\delta T_{mm}. \tag{2.26}$$

Similarly, the eigenfrequencies, ω'_m, and eigenvectors, $\mathbf{c}'_m$, of the modified operators, $\mathbf{T}'$ and $\mathbf{H}'$, are solutions of

$$(\omega_m'^2\mathbf{T}' - \mathbf{H}')\mathbf{c}'_m = 0. \tag{2.27}$$

The errors of the eigenfrequencies of the modified operators $\delta\omega' = \omega'_m - \omega_m^{(0)}$ can be found as shown above, but we also use eq. (2.20) to obtain

$$2\omega_m^{(0)}\delta\omega'_m = \delta H'_{mm} - \omega_m^{(0)^2}\delta T'_{mm} \approx 0. \tag{2.28}$$

Thus eq. (2.20), which we derived by minimizing the error of the numerical solution, is equivalent to requiring the error of the eigenfrequencies of the modified operators to be approximately equal to zero. Since the modes are a complete set, the sum of all the modes yields a complete synthetic seismogram. If the eigenfrequencies are all accurate to some given order, the velocity of *P* and *S* waves in the numerical solutions will be accurate to the same order. Thus we suppress numerical dispersion as a consequence of reducing the error of the numerical solutions.

It might seem intuitively reasonable to think that the errors of the numerical solutions will be largest where the errors of the numerical operators are largest. However, this is not the case. As shown by eqs (2.16) and (2.18), the spatial pattern of the error of the numerical solution in the vicinity of $\omega = \omega_m$ is given by the eigenfunction of the *m*th mode. A large numerical error of the operators near a free surface or internal discontinuity does not mean that the error of the numerical solution will be unusually large there; it simply means that the scalar quantity

$$\frac{\omega^2\delta T_{mm} - \delta H_{mm}}{\omega^2 - \omega_m^2},$$

which, as shown by eq. (2.20), is the factor controlling the relative error of the expansion coefficient of the *m*th mode in the vicinity of $\omega = \omega_m$, will be somewhat larger. This means that the relative error of the numerical solution will be uniformly larger everywhere in the medium, rather than that the error will be especially large at some particular points. Thus we do not have to be especially concerned with reducing the error of the operators at particular points, even points where we particularly desire accurate solutions.

3 *SH* PROBLEM

As the methods used to reduce the laterally homogeneous *SH* problem to a 1-D problem are standard, we do not discuss them here. The strong form of the equation of motion for the laterally homogeneous *SH* problem (Fig. 1a) in the (ω, k_x, z) domain is as follows:

$$(\rho\omega^2 - k_x^2\mu)u + \frac{d}{dz}\left(\mu\frac{du}{dz}\right) = -f, \tag{3.1}$$

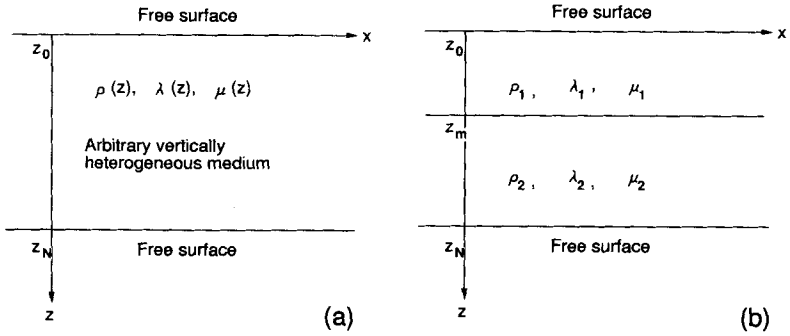

Figure 1. (a) The medium for the laterally homogeneous problem. The density, ρ, and Lamé constants, λ and μ, are functions of depth only. (b) Two-layered model for the laterally homogeneous problem. ρ_1 and ρ_2 are the densities in region 1 and region 2, respectively, λ_1, λ_2, μ_1 and μ_2 are the Lamé constants in each region.

where u and f are the depth-dependent parts of the y-component of the displacement and the body force, respectively, ρ is the density, μ is the rigidity, which includes the effect of anelastic attenuation (e.g. Liu, Anderson & Kanamori 1976), and k_x is the x-component of the wavenumber vector. The following discussion is also applicable to problems in cylindrical coordinates, since the vertically dependent part of the equation of motion is the same as for the Cartesian case. The weak form of the equation of motion for a medium with free surface natural boundary conditions is

$$\int_{z_0}^{z_N} [X_m(\rho\omega^2 - k_x^2\mu)u - X'_m\mu u'] \, dz = -\int_{z_0}^{z_N} X_m f \, dz \qquad (m = 0, \ldots, N), \tag{3.2}$$

where X_m is a real trial function, and the prime denotes differentiation with respect to z.

We represent u as a linear combination of the trial functions,

$$u = \sum_{m=0}^{N} c_m X_m. \tag{3.3}$$

We use linear spline trial functions in the remainder of this paper (Fig. 2):

$$X_m(z) = \begin{cases} (z - z_{m-1})/(z_m - z_{m-1}) & z_{m-1} < z \le z_m, \\ (z_{m+1} - z)/(z_{m+1} - z_m) & z_m \le z < z_{m+1}, \\ 0 & \text{otherwise}. \end{cases} \tag{3.4}$$

We neglect the first line of eq. (3.4) for $m = 0$ and the second line for $m = N$.

The unmodified matrix and vector elements for the *SH* problem are as follows:

$$T_{mn} = \int_{z_0}^{z_N} X_m \rho X_n \, dz, \tag{3.5}$$

$$H_{mn} = k_x^2 H_{mn}^{(1)} + H_{mn}^{(2)}, \tag{3.6}$$

where

$$H_{mn}^{(1)} = \int_{z_0}^{z_N} X_m \mu X_n \, dz, \tag{3.7}$$

$$H_{mn}^{(2)} = \int_{z_0}^{z_N} X'_m \mu X'_n \, dz, \tag{3.8}$$

$$g_m = \int_{z_0}^{z_N} X_m f \, dz. \tag{3.9}$$

For trial functions of the form of eq. (3.4), the integrands of eqs (3.5), (3.7) and (3.8) will be non-zero only when $|m - n| \le 1$. Thus **T** and **H** are tridiagonal.

We define the following three bilinear integral operators based on the left-hand side of eq. (3.2):

$$T(X_m, u) = \int_{z_0}^{z_N} X_m \rho u \, dz, \tag{3.10}$$

$$H^{(1)}(X_m, u) = \int_{z_0}^{z_N} X_m \mu u \, dz, \tag{3.11}$$

$$H^{(2)}(X_m, u) = \int_{z_0}^{z_N} (X_m)_{,z} \mu u_{,z} \, dz. \tag{3.12}$$

We analyse the error of the operators in eqs (3.5)–(3.8) using a strong form treatment. We formally integrate eq. (3.12) by parts

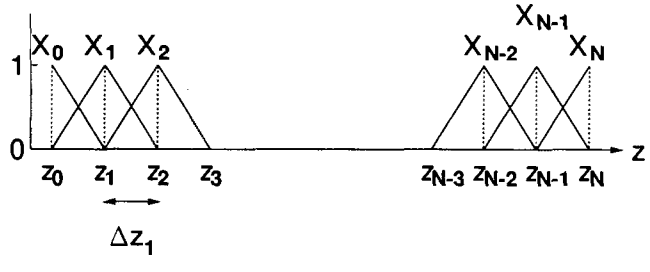

Figure 2. The linear spline functions $X_p(z)$. Note that the grid interval Δz_p is not necessarily constant.

to obtain either the operator 'to the right':

$$H^{(2)}(X_m, u) = X_m \mu u_{,z}|_{\text{DISCON}} - \int_{z_0}^{z_N} X_m(\mu u_{,z})_{,z}\, dz \tag{3.13}$$

or 'to the left':

$$H^{(2)}(X_m, u) = (X_m)_{,z} \mu u|_{\text{DISCON}} - \int_{z_0}^{z_N} [\mu (X_m)_{,z}]_{,z} u\, dz\,. \tag{3.14}$$

The integrations in eqs (3.13) and (3.14) are performed piecewise. For example, if there is a discontinuity in μ at $z = z_b$, the boundary terms in eqs (3.13) and (3.14) are $|_{z_0}^{z_b}$ and $|_{z_b}^{z_N}$, and the integrals $\int_{z_0}^{z_N}$ are evaluated as the sum of $\int_{z_0}^{z_b}$ and $\int_{z_b}^{z_N}$.

3.1 Homogeneous *SH*

The unmodified operators are obtained using eqs (3.5) and (3.6). We consider the case for which the grid interval Δz is constant. The explicit form of the unmodified operators is as follows:

$$\left.\begin{matrix}\mathbf{T} \\ \mathbf{H}^{(1)}\end{matrix}\right\} = \left.\begin{matrix}\rho \\ \mu\end{matrix}\right\} \Delta z \begin{bmatrix} 1/3 & 1/6 & & & & \\ 1/6 & 2/3 & 1/6 & & & \\ & \ddots & \ddots & \ddots & & \\ & & & 1/6 & 2/3 & 1/6 \\ & & & & 1/6 & 1/3 \end{bmatrix}, \tag{3.15}$$

$$\mathbf{H}^{(2)} = \frac{\mu}{\Delta z} \begin{bmatrix} 1 & -1 & & & & \\ -1 & 2 & -1 & & & \\ & \ddots & \ddots & \ddots & & \\ & & & -1 & 2 & -1 \\ & & & & -1 & 1 \end{bmatrix}. \tag{3.16}$$

$\mathbf{H}^{(2)}$ has the form of a finite-difference operator (e.g. Isaacson & Keller 1966, p. 293) for

$$-\left(\mu \frac{d^2u}{dz^2}\right) \Delta z\,.$$

Each of the expansion coefficients is equal to the displacement at the corresponding node. For convenience we set $z_0 = 0$ in this subsection. We can therefore write

$$\mathbf{c} = \begin{pmatrix} c_0 \\ c_1 \\ c_2 \\ \vdots \\ c_N \end{pmatrix} = \mathbf{u} = \begin{pmatrix} u(0) \\ u(\Delta z) \\ u(2\Delta z) \\ \vdots \\ u(N\Delta z) \end{pmatrix}. \tag{3.17}$$

We approximate the integrand in eq. (3.13) by its value at each node. The integral for the first node is taken from $z = 0$ to $z = \Delta z/2$, the integral for the second node from $z = \Delta z/2$ to $z = 3\Delta z/2, \ldots$, and the integral for the last node from $z = (2N-1)\Delta z/2$ to $z = N\Delta z$. We obtain from eq. (3.13)

$$\mathbf{H}^{(2)}_{\text{exact}}\mathbf{u} = -\mu\Delta z \begin{pmatrix} \frac{1}{2}u''(0) \\ u''(\Delta z) \\ u''(2\Delta z) \\ \vdots \\ u''((N-1)\Delta z) \\ \frac{1}{2}u''(N\Delta z) \end{pmatrix} + \mu \begin{pmatrix} -u'(0) \\ 0 \\ 0 \\ \vdots \\ 0 \\ u'(N\Delta z) \end{pmatrix}. \tag{3.18}$$

The first column vector in eq. (3.18) corresponds to the integral in eq. (3.13); the second column vector, which corresponds to the boundary term in eq. (3.13), does not depend on Δz.

We evaluate the exact operators $\mathbf{T}$ and $\mathbf{H}^{(1)}$ using the same approach as in eq. (3.18):

$$\left.\begin{matrix}\mathbf{T}_{\text{exact}}\mathbf{u}\\ \mathbf{H}^{(1)}_{\text{exact}}\mathbf{u}\end{matrix}\right\} = \left\{\begin{matrix}\rho\\ \mu\end{matrix}\right\} \Delta z \begin{pmatrix} \frac{1}{2}u(0) \\ u(\Delta z) \\ u(2\Delta z) \\ \vdots \\ u((N-1)\Delta z) \\ \frac{1}{2}u(N\Delta z) \end{pmatrix}. \tag{3.19}$$

To evaluate the errors of the numerical operators in eqs (3.15) and (3.16) we use the standard approach of expanding the terms of the right-hand column vector in a Taylor series:

$$u_{i-1} = u(z_i - \Delta z) = u - u'\Delta z + \tfrac{1}{2}u''(\Delta z)^2 - \tfrac{1}{6}u^{(3)}(\Delta z)^3 + \tfrac{1}{24}u^{(4)}(\Delta z)^4 - \cdots, \tag{3.20}$$

$$u_{i+1} = u(z_i + \Delta z) = u + u'\Delta z + \tfrac{1}{2}u''(\Delta z)^2 + \tfrac{1}{6}u^{(3)}(\Delta z)^3 + \tfrac{1}{24}u^{(4)}(\Delta z)^4 + \cdots, \tag{3.21}$$

where prime denotes differentiation, and all of the derivatives are evaluated at $z = z_i$. We also introduce two other expansions used below, in Section 4:

$$u_{i-2} = u - 2u'\Delta z + \frac{4u''(\Delta z)^2}{2} - \frac{8u^{(3)}(\Delta z)^3}{6} + \cdots, \tag{3.22}$$

$$u_{i+2} = u_i + 2u'\Delta z + \frac{4u''(\Delta z)^2}{2} + \frac{8u^{(3)}(\Delta z)^3}{6} + \cdots. \tag{3.23}$$

Using eqs (3.20) and (3.21), we obtain the following from eq. (3.16):

$$\mathbf{H}^{(2)}\mathbf{u} = [\mathbf{H}^{(2)}_{\text{exact}} + \delta\mathbf{H}^{(2)}]\mathbf{u}. \tag{3.24}$$

The lowest-order terms of the error are

$$\delta\mathbf{H}^{(2)}\mathbf{u} = -\mu\frac{\Delta z^3}{12}\begin{pmatrix} \frac{1}{2}u^{(4)}(0) \\ u^{(4)}(\Delta z) \\ u^{(4)}(2\Delta z) \\ \vdots \\ u^{(4)}((N-1)\Delta z) \\ \frac{1}{2}u^{(4)}(N\Delta z) \end{pmatrix} + \mu\frac{\Delta z^2}{6}\begin{pmatrix} -u^{(3)}(0) \\ 0 \\ 0 \\ \vdots \\ 0 \\ u^{(3)}(N\Delta z) \end{pmatrix}. \tag{3.25}$$

3.2 'Basic error' and 'boundary error'

Hereafter we denote error terms like the first column vector in eq. (3.25), which are present throughout the medium, as the 'basic error'. In contrast we denote terms like the second column vector in eq. (3.25), which contains error terms that arise only at external or internal boundaries, as the 'boundary error'. Using eqs (3.20) and (3.21), we obtain from eq. (3.15)

$$\mathbf{T}\mathbf{u} = (\mathbf{T}_{\text{exact}} + \delta\mathbf{T})\mathbf{u}, \tag{3.26}$$

$$\mathbf{H}^{(1)}\mathbf{u} = [\mathbf{H}^{(1)}_{\text{exact}} + \delta\mathbf{H}^{(1)}]\mathbf{u}, \tag{3.27}$$

where

$$\left.\begin{matrix}\delta\mathbf{T}\mathbf{u}\\ \delta\mathbf{H}^{(1)}\mathbf{u}\end{matrix}\right\} = \left\{\begin{matrix}\rho\\ \mu\end{matrix}\right\} \left[\frac{\Delta z^3}{6}\begin{pmatrix} \frac{1}{2}u''(0) \\ u''(\Delta z) \\ u''(2\Delta z) \\ \vdots \\ u''((N-1)\Delta z) \\ \frac{1}{2}u''(N\Delta z) \end{pmatrix} + \frac{\Delta z^2}{6}\begin{pmatrix} u'(0) \\ 0 \\ 0 \\ \vdots \\ 0 \\ -u'(N\Delta z) \end{pmatrix} \right]. \tag{3.28}$$

Using eqs (3.25) and (3.28), we obtain the following expression for the error:

$$(\omega^2\delta\mathbf{T}-\delta\mathbf{H})\mathbf{u}=\frac{\Delta z^3}{12}\begin{pmatrix}(\rho\omega^2-k_x^2\mu)u''(0)+\frac{1}{2}\mu u^{(4)}(0)\\2(\rho\omega^2-k_x^2\mu)u''(\Delta z)+\mu u^{(4)}(\Delta z)\\2(\rho\omega^2-k_x^2\mu)u''(2\Delta z)+\mu u^{(4)}(2\Delta z)\\\vdots\\2(\rho\omega^2-k_x^2\mu)u''((N-1)\Delta z)+\mu u^{(4)}((N-1)\Delta z)\\(\rho\omega^2-k_x^2\mu)u''(N\Delta z)+\frac{1}{2}\mu u^{(4)}(N\Delta z)\end{pmatrix}+\frac{\Delta z^2}{6}\begin{pmatrix}(\rho\omega^2-k_x^2\mu)u'(0)+\mu u^{(3)}(0)\\0\\\vdots\\0\\-(\rho\omega^2-k_x^2\mu)u'(N\Delta z)-\mu u^{(3)}(N\Delta z)\end{pmatrix}. \tag{3.29}$$

When $\mathbf{u}$ is an eigenfunction an ω is the corresponding eigenfrequency, the basic error at each node (except for the factor of 1/2 at the boundary nodes) in eq. (3.29) has the form

$$\frac{\Delta z^3}{12}[2(\rho\omega^2-k_x^2\mu)u''+\mu u^{(4)}]=\frac{\Delta z^3}{12}\{(\rho\omega^2-k_x^2\mu)u''+[(\rho\omega^2-k_x^2\mu)u+\mu u'']''\}=\frac{\Delta z^3}{12}(\rho\omega^2-k_x^2\mu)u''\neq 0, \tag{3.30}$$

where we used eq. (3.1) to show that the bracketed term in the second line of eq. (3.30) is zero to $O(\Delta z^2)$.

3.3 Modified operators

We define the following modified matrix operators:

$$\left.\begin{matrix}\mathbf{T}'\\\mathbf{H}^{(1)'}\end{matrix}\right\}=\left.\begin{matrix}\rho\\\mu\end{matrix}\right\}\Delta z\begin{bmatrix}5/12 & 1/12 & & & \\ 1/12 & 5/6 & 1/12 & & \\ & \ddots & \ddots & \ddots & \\ & & 1/12 & 5/6 & 1/12\\ & & & 1/12 & 5/12\end{bmatrix}, \tag{3.31}$$

The errors of the modified operators $\delta\mathbf{T}'=\mathbf{T}'-\mathbf{T}_{\text{exact}}$ and $\delta\mathbf{H}^{(1)'}=\mathbf{H}^{(1)'}-\mathbf{H}^{(1)}_{exact}$ are

$$\left.\begin{matrix}\delta\mathbf{T}'\mathbf{u}\\\delta H^{(1)'}\mathbf{u}\end{matrix}\right\}=\left.\begin{matrix}\rho\\\mu\end{matrix}\right\}\left[\frac{\Delta z^3}{12}\begin{pmatrix}\frac{1}{2}u''(0)\\u''(\Delta z)\\u''(2\Delta z)\\\vdots\\u''[(N-1)\Delta z]\\\frac{1}{2}u''(N\Delta z)\end{pmatrix}+\frac{\Delta z^2}{12}\begin{pmatrix}u'(0)\\0\\0\\\vdots\\0\\-u'(N\Delta z)\end{pmatrix}\right]. \tag{3.32}$$

The operator $\mathbf{H}^{(2)}$ is not modified. Thus the modified stiffness matrix is

$$\mathbf{H}'=k_x^2\mathbf{H}^{(1)\prime}+\mathbf{H}^{(2)}. \tag{3.33}$$

We combine eqs (3.25) and (3.23) to obtain

$$(\omega^2\delta\mathbf{T}'-\delta\mathbf{H}')\mathbf{u}=\frac{\Delta z^3}{12}\begin{pmatrix}\frac{1}{2}[(\rho\omega^2-k_x^2\mu)u''(0)+\mu u^{(4)}(0)]\\(\rho\omega^2-k_x^2\mu)u''(\Delta z)+\mu u^{(4)}(\Delta z)\\\vdots\\(\rho\omega^2-k_x^2\mu)u''((N-1)\Delta z)+\mu u^{(4)}((N-1)\Delta z)\\\frac{1}{2}[(\rho\omega^2-k_x^2\mu)u''(N\Delta z)+\mu u^{(4)}(N\Delta z)]\end{pmatrix}+\frac{\Delta z^2}{12}\begin{pmatrix}(\rho\omega^2-k_x^2\mu)u'(0)+2\mu u^{(3)}(0)\\0\\\vdots\\0\\-(\rho\omega^2-k_x^2\mu)u'(N\Delta z)-2\mu u^{(3)}(N\Delta z)\end{pmatrix}. \tag{3.34}$$

When ω is equal to the eigenfrequency of the mode for which $\mathbf{u}$ is the eigenfunction, the basic error at each node point (the elements of the first vector on the right-hand side of eq. (3.34) is zero to $O(\Delta z^2)$. The modified operator $(\omega^2\mathbf{T}'-\mathbf{H}')$ thus approximately satisfies eqs (2.20), (2.23) and (2.24).

We define the wave velocities and the vertical components of the wavenumbers. The results for P waves will be used in the next

section. We have

$$\alpha = \sqrt{\frac{\lambda + 2\mu}{\rho}}, \qquad \beta = \sqrt{\frac{\mu}{\rho}}, \tag{3.35}$$

$$k_{z\alpha}^2 = \frac{\omega^2}{\alpha^2} - k_x^2, \qquad k_{z\beta}^2 = \frac{\omega^2}{\beta^2} - k_x^2. \tag{3.36}$$

Eq. (3.32) gives the basic error component of $\delta\mathbf{T}'$ as

$$\frac{\rho\Delta z^3}{12} u'' = -\frac{\rho\Delta z^3}{12} k_{z\beta}^2 u, \tag{3.37}$$

where we used eq. (3.1). If u is an eigenfunction, it is normalized such that

$$[u^*(0), u^*(\Delta z), \ldots, u^*(N\Delta z)]\rho\Delta z \begin{pmatrix} \frac{1}{2}u(0) \\ u(\Delta z) \\ u(2\Delta z) \\ \vdots \\ u((N-1)\Delta z) \\ \frac{1}{2}u(N\Delta z) \end{pmatrix} = 1. \tag{3.38}$$

We combine eqs (2.21), (3.32), (3.37) and (3.38) to obtain the relative error (see eq. 2.21)

$$|\delta T_{mm}| = \left| \frac{k_{z\beta}^2 \Delta z^2}{12} \right|. \tag{3.39}$$

3.4 Inhomogeneous *SH*(1)

We use a constant grid interval in each region (Δz_1 in region 1 and Δz_2 in region 2) in this example. The operators for the inhomogeneous medium shown in Fig. 1(b) are obtained by 'overlapping' as shown in Fig. 3(a):

$$\mathbf{H}^{(1)'} = \begin{bmatrix} \ddots & \ddots & & & & & \\ \ddots & \ddots & \ddots & & & & \\ (1/12)\mu_1\Delta z_1 & (5/6)\mu_1\Delta z_1 & (1/12)\mu_1\Delta z_1 & & & & \\ & (1/12)\mu_1\Delta z_1 & (5/12)(\mu_1\Delta z_1 + \mu_2\Delta z_2) & (1/12)\mu_2\Delta z_2 & & & \\ & & (1/12)\mu_2\Delta z_2 & (5/6)\mu_2\Delta z_2 & \ddots & & \\ & & & \ddots & \ddots & & \end{bmatrix} \tag{3.40}$$

$$\mathbf{H}^{(2)} = \begin{bmatrix} \ddots & \ddots & & & & & \\ \ddots & \ddots & \ddots & & & & \\ -\frac{\mu_1}{\Delta z_1} & 2\frac{\mu_1}{\Delta z_1} & -\frac{\mu_1}{\Delta z_1} & & & & \\ & -\frac{\mu_1}{\Delta z_1} & \frac{\mu_1}{\Delta z_1} + \frac{\mu_2}{\Delta z_2} & -\frac{\mu_2}{\Delta z_2} & & & \\ & & -\frac{\mu_2}{\Delta z_2} & 2\frac{\mu_2}{\Delta z_2} & \ddots & & \\ & & & \ddots & \ddots & & \end{bmatrix} \tag{3.41}$$

$$\mathbf{T}' = \begin{bmatrix} \ddots & \ddots & & & & & \\ \ddots & \ddots & \ddots & & & & \\ (1/12)\rho_1\Delta z_1 & (5/6)\rho_1\Delta z_1 & (1/12)\rho_1\Delta z_1 & & & & \\ & (1/12)\rho_1\Delta z_1 & (5/12)(\rho_1\Delta z_1 + \rho_2\Delta z_2) & (1/12)\rho_2\Delta z_2 & & & \\ & & (1/12)\rho_2\Delta z_2 & (5/6)\rho_2\Delta z_2 & \ddots & & \\ & & & \ddots & \ddots & & \end{bmatrix}. \tag{3.42}$$

The modified operators in eqs (3.40)–(3.42) are equivalent to those used by Korn (1987).

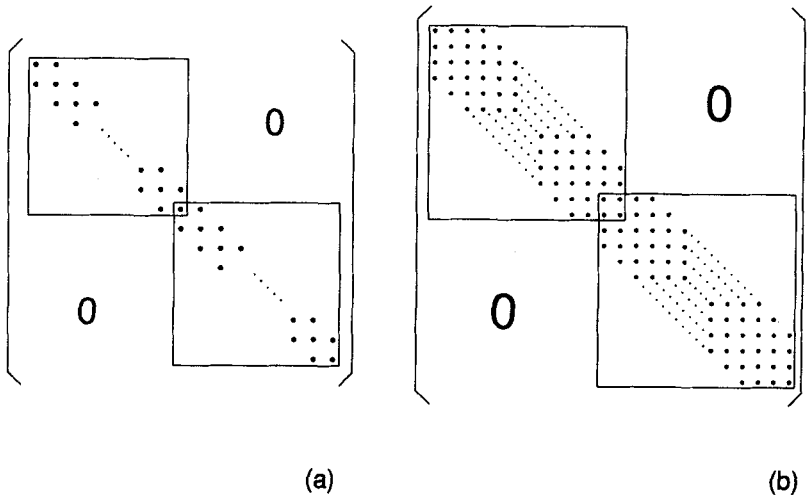

Figure 3. (a) The *SH* stiffness and mass matrices for the two-layered medium in Fig. 1(b) are constructed by overlapping operators for the respective media as shown. The overlapped element is summed. (b) The modified *P-SV* mass and stiffness matrices for the two-layered medium shown in Fig. 1(b) are constructed by overlapping operators for the respective media as shown. The overlapped elements are summed. Note that the matrix elements in the third supra- and sub-diagonals are zero where the matrices are overlapped.

We use a straightforward extension of the procedure used to derive eq. (3.34) to obtain the error of $(\omega^2\mathbf{T}' - \mathbf{H}')$. The basic error for each mode is zero to $O(\Delta z^2)$ when ω is equal to that mode's eigenfrequency; the boundary error is

$$(\omega^2\boldsymbol{\delta}\mathbf{T}' - \boldsymbol{\delta}\mathbf{H}')\mathbf{u} = \begin{bmatrix} \frac{\Delta z_1^2}{12}[(\rho_1\omega^2 - k_x^2\mu_1)u'(z_0) + 2\mu_1 u^{(3)}(z_0)] \\ 0 \\ \vdots \\ 0 \\ -\frac{\Delta z_1^2}{12}[(\rho_1\omega^2 - k_x^2\mu_1)u'(z_m^-) + 2\mu_1 u^{(3)}(z_m^-)] + \frac{\Delta z_2^2}{12}[(\rho_2\omega^2 - k_x^2\mu_2)u'(z_m^+) + 2\mu_2 u^{(3)}(z_m^+)] \\ 0 \\ \vdots \\ 0 \\ -\frac{\Delta z_2^2}{12}[(\rho_2\omega^2 - k_x^2\mu_2)u'(z_N) + 2\mu_2 u^{(3)}(z_N)] \end{bmatrix}. \tag{3.43}$$

Thus the modified operators approximately satisfy eq. (2.23) to $O(\Delta z^2)$. Because of the nature of the eigenfunctions, the first and last elements of the vector in eq. (3.43) will fortuitously be zero, but the boundary error at the internal boundary at $z = z_m$ will in general be non-zero.

3.5 Inhomogeneous *SH*(2)

We consider the case in which μ and ρ are inhomogeneous but have no discontinuities, and Δz is constant. If there are discontinuities in elastic properties or Δz, separate operators can be constructed for each segment and then overlapped as shown in Fig. 3(a). We divide the density and elastic properties into two parts: one varying step-wise in each segment centred around a node and the residual, which can vary arbitrarily. Using μ as an example, and setting $z_0 = 0$ for convenience, we define

$$(\mu_{\text{step}})_j = \begin{cases} \frac{2}{\Delta z}\int_0^{\Delta z/2} \mu\, dz & (j=0), \\ \frac{1}{\Delta z}\int_{(j-1/2)\Delta z}^{(j+1/2)\Delta z} \mu\, dz & (1 \le j \le N-1), \\ \frac{2}{\Delta z}\int_{(N-1/2)\Delta z}^{N\Delta z} \mu\, dz & (j=N), \end{cases} \tag{3.44}$$

$$\mu_{\text{resid}} = \mu - (\mu_{\text{step}})_j \qquad \text{for } (j-1/2)\Delta z \le z < (j+1/2)\Delta z. \tag{3.45}$$

We neglect $z < 0$ and $z > N\Delta z$ in eq. (3.45). We similarly define $(\lambda_{\text{step}})_j$ and λ_{resid}, and $(\rho_{\text{step}})_j$ and ρ_{resid}, by replacing μ by λ and ρ, respectively, in eqs (3.44) and (3.45).

We divide the modified operators into two parts:

$$\mathbf{T}' = \mathbf{T}'_{\text{step}} + \mathbf{T}_{\text{resid}} \tag{3.46}$$

$$\mathbf{H}' = \mathbf{H}'_{\text{step}} + \mathbf{H}_{\text{resid}} \tag{3.47}$$

As we assume ρ_{resid} and μ_{resid} are relatively small, we account for their effects using the unmodified operators in eqs (3.5) and (3.6).

We consider $\mathbf{H}'_{\text{step}}$ and $\mathbf{T}'_{\text{step}}$ in the following discussion, but we drop the subscript 'step' from both the operators and elastic moduli. The density and rigidity at the jth grid point are $\rho_j = \rho(j\Delta z)$ and $\mu_j = \mu(j\Delta z)$, respectively, as given by eq. (3.44). $\mathbf{H}^{(2)}$ is obtained using eq. (3.8):

$$\mathbf{H}^{(2)} = \frac{1}{2\Delta z}\begin{bmatrix} \mu_0+\mu_1 & -(\mu_0+\mu_1) & & & & \\ -(\mu_0+\mu_1) & \mu_0+2\mu_1+\mu_2 & -(\mu_1+\mu_2) & & & \\ & \ddots & \ddots & \ddots & & \\ & & -(\mu_{N-2}+\mu_{N-1}) & \mu_{N-2}+2\mu_{N-1}+\mu_N & -(\mu_{N-1}+\mu_N) & \\ & & & -(\mu_{N-1}+\mu_N) & \mu_{N-1}+\mu_N \end{bmatrix}. \tag{3.48}$$

We define the modified 'mass matrix to the right' as follows:

$$\mathbf{T}'_{\text{right}} = \Delta z\begin{bmatrix} \frac{5}{12}\rho_0 & \frac{1}{12}\rho_0 & & & & \\ \frac{1}{12}\rho_1 & \frac{5}{6}\rho_1 & \frac{1}{12}\rho_1 & & & \\ & \frac{1}{12}\rho_2 & \frac{5}{6}\rho_2 & \frac{1}{12}\rho_2 & & \\ & & \ddots & \ddots & \ddots & \\ & & & \frac{1}{12}\rho_{N-1} & \frac{5}{6}\rho_{N-1} & \frac{1}{12}\rho_{N-1} \\ & & & & \frac{1}{12}\rho_N & \frac{5}{12}\rho_N \end{bmatrix}. \tag{3.49}$$

Any arbitrary linear combination of $\mathbf{T}'_{\text{right}}$ and $\mathbf{T}'^{\text{T}}_{\text{right}}$ with weights summing to one could be used as the mass matrix without significantly degrading the accuracy of the numerical solutions. We use the symmetric part of $\mathbf{T}'_{\text{right}}$,

$$\mathbf{T}' = \tfrac{1}{2}(\mathbf{T}'_{\text{right}} + \mathbf{T}'^{\text{T}}_{\text{right}}), \tag{3.50}$$

as the modified mass matrix to ensure that reciprocity will be satisfied by the numerical solutions.

We define the modified operator 'to the right', $\mathbf{H}^{(1)'}_{\text{right}}$, as follows:

$$\mathbf{H}^{(1)'}_{\text{right}} = \Delta z\begin{bmatrix} \frac{5}{12}\mu_0 & \frac{1}{12}\mu_0 & & & & \\ \frac{1}{12}\mu_1 & \frac{5}{6}\mu_1 & \frac{1}{12}\mu_1 & & & \\ & \frac{1}{12}\mu_2 & \frac{5}{6}\mu_2 & \frac{1}{12}\mu_2 & & \\ & & \ddots & \ddots & \ddots & \\ & & & \frac{1}{12}\mu_{N-1} & \frac{5}{6}\mu_{N-1} & \frac{1}{12}\mu_{N-1} \\ & & & & \frac{1}{12}\mu_N & \frac{5}{12}\mu_N \end{bmatrix}, \tag{3.51}$$

and use the symmetric part of $\mathbf{H}^{(1)'}_{\text{right}}$ as $\mathbf{H}^{(1)'}$:

$$\mathbf{H}^{(1)'} = \tfrac{1}{2}[\mathbf{H}^{(1)'}_{\text{right}} + \mathbf{H}^{(1)'^{\text{T}}}_{\text{right}}]. \tag{3.52}$$

The modified stiffness matrix $\mathbf{H}'$ is given by eq. (3.33), using eqs (3.48) and (3.52). Note that eqs (3.50) and (3.52) reduce to eq. (3.31) for a homogeneous medium.

A straightforward analysis using Taylor series expansions of both u and μ shows that the operator $\mathbf{H}^{(2)}$ in eq. (3.48) has the following value (first term) and basic error (second term):

$$-\Delta z(\mu u')' - \frac{\Delta z^3}{12}[\mu u^{(4)} + 2\mu' u^{(3)} + 3\mu'' u'' + 2\mu^{(3)} u'']. \tag{3.53}$$

On the other hand, the desired value (first term) and basic error (second term) are

$$-\Delta z(\mu u')' - \frac{\Delta z^3}{12}[(\mu u')']'' = -\Delta z(\mu u')' - \frac{\Delta z^3}{12}[\mu u^{(4)} + 3\mu' u^{(3)} + 3\mu'' u'' + \mu^{(3)} u']. \tag{3.54}$$

However, we are most concerned with the accuracy when k_z is largest. In this case μ' and the higher derivatives of the elastic moduli will be negligible, so we can regard the basic error in eq. (3.53) as fully acceptable for practical purposes.

Eq. (3.50) gives the modified operator $\mathbf{T}'$. A Taylor series expansion considering the derivatives of both u and ρ gives the following value and basic error:

$$\rho u + \frac{\Delta z^2}{12}(\rho u'' + \rho' u' + \tfrac{1}{2}\rho'' u), \tag{3.55}$$

whereas the desired value and basic error are

$$\rho u + \frac{\Delta z^2}{12}(\rho u)'' = \rho u + \frac{\Delta z^2}{12}(\rho u'' + 2\rho' u' + \rho'' u). \tag{3.56}$$

The value and basic error of $\mathbf{H}^{(1)'}$ are obtained by replacing ρ by μ in eqs (3.55) and (3.56). In summary, the modified operators in eqs (3.50) and (3.52) approximately satisfy eq. (2.24) with sufficient accuracy to $O(\Delta z^2)$.

3.6 Absorbing boundary conditions

We consider a medium with a free boundary at $z = z_0$, and the following radiation boundary condition at $z = z_N$:

$$\frac{du}{dz} + ik_{\beta z} u = 0. \tag{3.57}$$

As shown by Geller & Ohminato (1994, eqs 9 and 37), the weak form operator for a medium with a radiation boundary condition is obtained by adding a surface integral to the weak form operator to alter the natural boundary condition. For the *SH* case with the boundary condition eq. (3.57), the weak form of the equation of motion is

$$\int_{z_0}^{z_N} [X_m(\rho\omega^2 - k_x^2\mu)u - (X_m)_{,z}\mu u_{,z}]\, dz - ik_{z\beta}\mu X_m u|_{z=z_N} = -\int_{z_0}^{z_N} X_m f\, dz \qquad (m = 0, 1, 2, \ldots, N). \tag{3.58}$$

The DSM equation of motion obtained from eq. (3.58) is

$$(\omega^2\mathbf{T} - \mathbf{H} + \mathbf{R})\mathbf{c} = -\mathbf{g}, \tag{3.59}$$

where $\mathbf{T}$, $\mathbf{H}$ and $\mathbf{g}$ are defined as in eqs (3.5)–(3.9), and $\mathbf{R}$ is given by

$$R_{mn} = -ik_{z\beta}\mu X_m X_n|_{z=z_N}. \tag{3.60}$$

It is straightforward to obtain modified operators for this case. We use $\mathbf{T}'$ as defined by eq. (3.50), and $\mathbf{H}'$ as defined by eq. (3.33). We define $\mathbf{R}'$ as follows:

$$R'_{mn} = -\left(1 - \frac{k_{z\beta}^2\Delta z^2}{12}\right) ik_{z\beta}\mu X_m X_n\Big|_{z=z_N}. \tag{3.61}$$

We can use the same approach for the *P-SV* case. The matrix elements for a radiation boundary condition are given by eqs (B15) and (B18) of Geller & Ohminato (1994).

If the rhs of eq. (3.59) is zero, it is a generalized eigenvalue problem (Lancaster 1966, ch. 4), as it contains ω^2, ω^1, and ω^0 terms. The formal error analysis in Section 2 is thus not directly applicable to eq. (3.59). We have not yet carried out a formal error analysis for eq. (3.59), but we conjecture it would lead to a criterion which is a generalization of eq. (2.20), and that the modified operators derived above for the *SH* problem with a radiation boundary condition could be shown to satisfy this generalized criterion.

4 *P-SV* PROBLEM

The strong form of the equation of motion for the laterally homogeneous *P-SV* problem (Fig. 1a) in the (ω, k_x, z) domain is

$$[\rho\omega^2 - \mu k_x^2]u_z - i\mu k_x \frac{du_x}{dz} + \frac{d}{dz}\left[-ik_x\lambda u_x + (\lambda + 2\mu)\frac{du_z}{dz}\right] + f_z = 0 \tag{4.1}$$

$$[\rho\omega^2 - (\lambda + 2\mu)k_x^2]u_x - i\lambda k_x \frac{du_z}{dz} + \frac{d}{dz}\left[\mu\left(\frac{du_x}{dz} - ik_x u_z\right)\right] + f_x = 0, \tag{4.2}$$

where u_z and u_x are the z-dependent parts of the z- and x-components of the displacement, and f_z and f_x are the z-dependent parts of the z- and x-components of the body force. The weak form of the equation of motion for a medium with free surface boundary conditions is

$$\int_{z_0}^{z_N} [X_p(\rho\omega^2 - \mu k_x^2)u_z - X_p ik_x\mu u'_x + X'_p ik_x\lambda u_x - X'_p(\lambda + 2\mu)u'_z]\, dz = -\int X_p f_z\, dz \qquad (p = 0, \cdots, N), \tag{4.3}$$

$$\int_{z_0}^{z_N} \{X_p[\rho\omega^2 - (\lambda + 2\mu)k_x^2]u_x - X_p ik_x\lambda u'_z + X'_p ik_x\mu u_z - X'_p\mu u'_x\}\, dz = -\int X_p f_x\, dz \qquad (p = 0, \cdots, N). \tag{4.4}$$

The trial function expansions and force vector elements are, respectively,

$$u_z = \sum_{p=0}^{N} c_{p1} X_p, \tag{4.5}$$

$$u_x = \sum_{p=0}^{N} c_{p2} X_p, \tag{4.6}$$

$$g_{p1} = \int_{z_0}^{z_N} f_z X_p \, dz, \tag{4.7}$$

$$g_{p2} = \int_{z_0}^{z_N} f_x X_p \, dz, \tag{4.8}$$

where $c_{p\gamma}$ is the expansion coefficient. The index $\gamma = 1$ denotes the z-component and $\gamma = 2$ denotes the x-component. The rows and columns of $\mathbf{T}$ and $\mathbf{H}$ and the elements of $\mathbf{c}$ and $\mathbf{g}$ are ordered so that γ varies most rapidly. We thus have the order $(p\gamma) = (01), (02), (11), (12), \cdots, (N1), (N2)$. We use $p\gamma$ as the indices for the rows of $\mathbf{T}$ and $\mathbf{H}$, and $p'\gamma'$ as the indices for the columns (see Fig. 4). $\mathbf{T}$ and $\mathbf{H}$ are given by

$$T_{p\gamma p'\gamma'} = \begin{cases} T^{(1)}_{pp'} & (\gamma = \gamma'), \\ 0 & \text{otherwise}, \end{cases} \tag{4.9}$$

$$H_{p\gamma p'\gamma'} = \begin{cases} k_x^2 H^{(2)}_{pp'} + H^{(5)}_{pp'} + 2H^{(6)}_{pp'} & (\gamma = \gamma' = 1), \\ -ik_x H^{(3)}_{p'p} + ik_x H^{(4)}_{pp'} & (\gamma = 1, \gamma' = 2), \\ ik_x H^{(3)}_{pp'} - ik_x H^{(4)}_{p'p} & (\gamma = 2, \gamma' = 1), \\ k_x^2 [H^{(1)}_{pp'} + 2H^{(2)}_{pp'}] + H^{(6)}_{pp'} & (\gamma = \gamma' = 2). \end{cases} \tag{4.10}$$

Note that some of the subscripts in the second and third rows of eq. (4.10) are in reverse order.

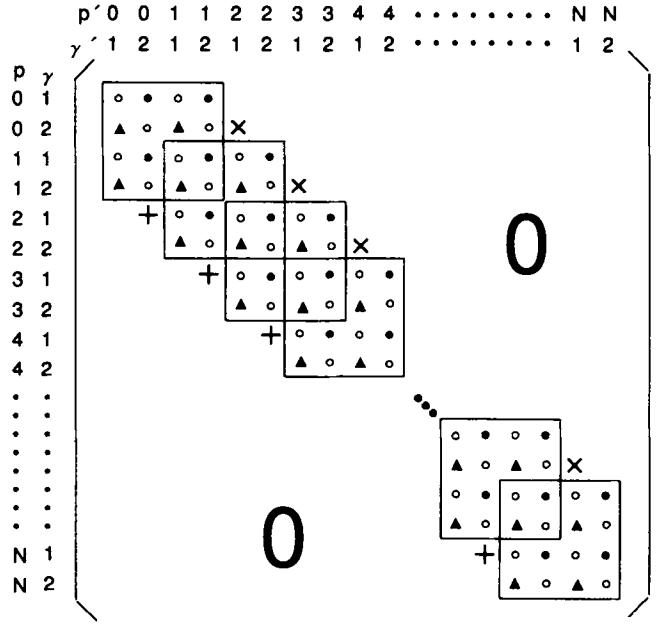

Figure 4. *P-SV* coefficient matrix ($\omega^2\mathbf{T} - \mathbf{H}$). $\mathbf{T}^{(1)}$, $\mathbf{H}^{(1)}$, $\mathbf{H}^{(2)}$, $\mathbf{H}^{(5)}$ and $\mathbf{H}^{(6)}$ contribute to the elements shown as open circles. $\mathbf{H}^{(3)}$ and $\mathbf{H}^{(4)\mathrm{T}}$ contribute to the matrix elements shown as black triangles. $\mathbf{H}^{(3)\mathrm{T}}$ and $\mathbf{H}^{(4)}$ contribute to the matrix elements shown as closed circles. The crosses indicate matrix elements which are zero for the original operators, but which we use for the modified operators $\mathbf{H}^{(3)'}$ and $\mathbf{H}^{(4)'\mathrm{T}}$. The plus signs indicate matrix elements which are zero for the original operators but which we use for the modified operators $\mathbf{H}^{(3)\mathrm{T}}$ and $\mathbf{H}^{(4)'}$. The use of these elements (crosses and pluses) does not increase the bandwidth of the coefficient matrix, and therefore does not increase the CPU time required to solve the DSM equation of motion, eq. (2.1). The numbering conventions for the rows and columns are shown at left and top, respectively.

The operators on the rhs of eq. (4.10), which we call 'submatrices', are

$$T^{(1)}_{pp'} = \int_{z_0}^{z_N} \rho X_p X_{p'}\, dz\,, \tag{4.11}$$

$$H^{(1)}_{pp'} = \int_{z_0}^{z_N} \lambda X_p X_{p'}\, dz\,, \tag{4.12}$$

$$H^{(2)}_{pp'} = \int_{z_0}^{z_N} \mu X_p X_{p'}\, dz\,, \tag{4.13}$$

$$H^{(3)}_{pp'} = \int_{z_0}^{z_N} \lambda X_p X'_{p'}\, dz\,, \tag{4.14}$$

$$H^{(4)}_{pp'} = \int_{z_0}^{z_N} \mu X_p X'_{p'}\, dz\,, \tag{4.15}$$

$$H^{(5)}_{pp'} = \int_{z_0}^{z_N} \lambda X'_p X'_{p'}\, dz\,, \tag{4.16}$$

$$H^{(6)}_{pp'} = \int_{z_0}^{z_N} \mu X'_p X'_{p'}\, dz\,. \tag{4.17}$$

$\mathbf{H}^{(3)}$ and $\mathbf{H}^{(4)^{\mathrm{T}}}$ contribute to the elements shown as black dots in Fig. 4, while $\mathbf{H}^{(3)^{\mathrm{T}}}$ and $\mathbf{H}^{(4)}$ contribute to the elements shown as black triangles. On the other hand $\mathbf{T}^{(1)}$, $\mathbf{H}^{(1)}$, $\mathbf{H}^{(2)}$, $\mathbf{H}^{(5)}$ and $\mathbf{H}^{(6)}$ contribute to the elements shown by open circles in Fig. 4.

For a homogeneous medium with constant Δz, $\mathbf{H}^{(3)}$ and $\mathbf{H}^{(4)}$ are as follows:

$$\left.\begin{matrix}\mathbf{H}^{(3)}\\ \mathbf{H}^{(4)}\end{matrix}\right\} = \left.\begin{matrix}\lambda\\ \mu\end{matrix}\right\} \begin{pmatrix} -1/2 & 1/2 & & & \\ -1/2 & 0 & 1/2 & & \\ & \ddots & \ddots & \ddots & \\ & & -1/2 & 0 & 1/2 \\ & & & -1/2 & 1/2 \end{pmatrix}. \tag{4.18}$$

$\mathbf{T}^{(1)}$, $\mathbf{H}^{(1)}$ and $\mathbf{H}^{(2)}$ are given by eq. (3.31) and $\mathbf{H}^{(5)}$ and $\mathbf{H}^{(6)}$ by eq. (3.16), with μ replaced by λ as appropriate.

We next consider a medium in which λ, μ, and ρ vary smoothly, and Δz is constant. Following the *SH* case, we divide the modified operators into two parts:

$$\mathbf{T}' = \mathbf{T}'_{\mathrm{step}} + \mathbf{T}_{\mathrm{resid}} \tag{4.19}$$

$$\mathbf{H}' = \mathbf{H}'_{\mathrm{step}} + \mathbf{H}_{\mathrm{resid}} \tag{4.20}$$

We use the unmodified operators in eqs (4.9)–(4.17) for ρ_{resid}, λ_{resid} and μ_{resid}. We now derive the modified operators for ρ_{step}, λ_{step} and μ_{step}. We drop the subscript 'step'.

The modified operators $\mathbf{T}^{(1)'}$, $\mathbf{H}^{(1)'}$ and $\mathbf{H}^{(2)'}$ have the same form as the modified operators in eq. (3.31). We now derive the modified operators $\mathbf{H}^{(3)'}$ and $\mathbf{H}^{(4)'}$. As discussed above (see eqs 1.4 and 1.5), the coefficients of the four-point operators can be chosen in a straightforward fashion to yield the desired basic error. We define the following bilinear operator based on the left-hand side of eq. (4.4):

$$H^{(3)}(X_p, u_z) = \int_{z_0}^{z_N} X_p \lambda u'_z\, dz\,. \tag{4.21}$$

Eq. (4.21) yields the operator to the right by inspection, as X_p is factored out in the integrand. We obtain the operator 'to the left' by formally integrating eq. (4.21) by parts:

$$H^{(3)}(X_p, u_z) = X_p \lambda u_z|_{\mathrm{DISCON}} - \int_{z_0}^{z_N} (X_p \lambda)_{,z} u_z\, dz\,. \tag{4.22}$$

Thus $\mathbf{H}^{(3)'}$ operating 'to the left' on $\mathbf{v}^{\mathrm{T}}$ should be a finite-difference operator for

$$-\frac{d}{dz}(\lambda v) + \lambda v|_{z_0}^{z_N}\,, \tag{4.23}$$

while $\mathbf{H}^{(3)'}$ operating to the right should be a finite-difference operator for

$$\lambda \frac{du}{dz}. \tag{4.24}$$

The modified operator $\mathbf{H}^{(3)'}$ is as follows:

$$\mathbf{H}^{(3)'}=\frac{1}{12}\begin{pmatrix} -7\lambda_0 & 8\lambda_0 & -\lambda_0 & & & & \\ -5\lambda_1 & -3\lambda_1 & 9\lambda_1 & -\lambda_1 & & & \\ & -5\lambda_2 & -3\lambda_2 & 9\lambda_2 & -\lambda_2 & & \\ & & \ddots & \ddots & \ddots & \ddots & \\ & & & -5\lambda_{N-1} & -3\lambda_{N-1} & 8\lambda_{N-1} \\ & & & & -5\lambda_N & 5\lambda_N \end{pmatrix}. \tag{4.25}$$

The first two terms in the top row and the last two terms in the rightmost column of the matrix in eq. (4.25) are chosen to match the boundary terms in eqs (4.24) and (4.25).

Using eqs (3.20)–(3.23), the value and error of the ith row of $\mathbf{H}^{(3)'}$ $(1 \le i \le N-2)$ are

$$\begin{aligned}[\mathbf{H}^{(3)'}\mathbf{u}]_i &= \lambda_i[-\tfrac{5}{12}u(z-\Delta z)-\tfrac{3}{12}u(z)+\tfrac{9}{12}u(z+\Delta z)-\tfrac{1}{12}u(z+2\Delta z)] \\ &= \lambda_i\left[\Delta z u'+\frac{\Delta z^3}{12}u^{(3)}+\cdots\right],\end{aligned} \tag{4.26}$$

where $\lambda_i \Delta z u'$ and $\lambda_i \Delta z^3 u^{(3)}/12$ are the exact value of the desired result and the basic error, respectively. In the $i=0$ row, $\mathbf{H}^{(3)'}$ has an $O(\Delta z^2)$ boundary error. For the $i=N-1$ and $i=N$ rows, $\mathbf{H}^{(3)'}$ has an $O(\Delta z)$ error, but, as shown below, the net contribution to $\mathbf{u}_m^*(\omega^2\boldsymbol{\delta}\mathbf{T}'-\boldsymbol{\delta}\mathbf{H}')\mathbf{u}_m$ is only $O(\Delta z^2)$:

$$\begin{aligned}\text{Contribution to } O(\Delta z) \text{ terms to } \mathbf{u}_m^*(\omega^2\boldsymbol{\delta}\mathbf{T}'-\boldsymbol{\delta}\mathbf{H}')\mathbf{u}_m &= \lambda_{N-1}u_x[(N-1)\Delta z]\{\tfrac{1}{12}u_z'((N-1)\Delta z)\Delta z\}+\lambda_N u_x(N\Delta z)[-\tfrac{1}{12}u_z'(N\Delta z)\Delta z] \\ &= O(\Delta z^2),\end{aligned}$$

where we expanded all of the quantities about $z=(N-1/2)\Delta z$ to prove eq. (4.27).

Omitting the details of the derivation, the modified operator, $\mathbf{H}^{(4)'}$ is as follows:

$$\mathbf{H}^{(4)'}=\frac{1}{12}\begin{pmatrix} -5\mu_0 & 5\mu_0 & & & & \\ -8\mu_1 & 3\mu_1 & 5\mu_1 & & & \\ \mu_2 & -9\mu_2 & 3\mu_2 & 5\mu_2 & & \\ & \ddots & \ddots & \ddots & \ddots & \\ & & \mu_{N-1} & -9\mu_{N-1} & 3\mu_{N-1} & 5\mu_{N-1} \\ & & & \mu_N & -8\mu_N & 7\mu_N \end{pmatrix}. \tag{4.28}$$

In summary, the modified operators for the *P-SV* problem are defined as follows:

$$T'_{p\gamma p'\gamma'}=\begin{cases} T^{(1)'}_{pp'} & (\gamma=\gamma'), \\ 0 & \text{otherwise}, \end{cases} \tag{4.29}$$

$$H'_{p\gamma p'\gamma'}=\begin{cases} k_x^2 H^{(2)'}_{pp'}+H^{(5)'}_{pp'}+2H^{(6)'}_{pp'} & (\gamma=\gamma'=1), \\ -ik_x H^{(3)'}_{p'p}+ik_x H^{(4)'}_{pp'} & (\gamma=1,\gamma'=2), \\ -ik_x H^{(4)'}_{p'p}+ik_x H^{(3)'}_{pp'} & (\gamma=2,\gamma'=1), \\ k_x^2[H^{(1)'}_{pp'}+2H^{(2)'}_{pp'}]+H^{(6)'}_{pp'} & (\gamma=\gamma'=2). \end{cases} \tag{4.30}$$

$\mathbf{H}^{(3)'}$ and $\mathbf{H}^{(4)'}$ are defined in eqs (4.25) and (4.28); $\mathbf{H}^{(5)}$ and $\mathbf{H}^{(6)}$ are defined by eqs (4.16) and (4.17). $\mathbf{T}^{(1)'}$, $\mathbf{H}^{(1)'}$ and $\mathbf{H}^{(2)'}$ are defined in the same way as eqs (3.50) and (3.33), replacing μ by λ where appropriate.

If the order of the u_x and u_z elements in $\mathbf{H}$ and $\mathbf{T}$ were reversed, we could derive the following modified operators $\mathbf{H}^{(3)''}$ and $\mathbf{H}^{(4)''}$ to replace the operators in eqs (4.25) and (4.28).

$$\mathbf{H}^{(3)''}=\frac{1}{12}\begin{pmatrix} -5\lambda_0 & 5\lambda_0 & & & & \\ -8\lambda_1 & 3\lambda_1 & 5\lambda_1 & & & \\ \lambda_2 & -9\lambda_2 & 3\lambda_2 & 5\lambda_2 & & \\ & \ddots & \ddots & \ddots & \ddots & \\ & & \lambda_{N-1} & -9\lambda_{N-1} & 3\lambda_{N-1} & 5\lambda_{N-1} \\ & & & \lambda_N & -8\lambda_N & 7\lambda_N \end{pmatrix}, \tag{4.31}$$

$$\mathbf{H}^{(4)''}=\frac{1}{12}\begin{pmatrix} -7\mu_0 & 8\mu_0 & -\mu_0 & & & & \\ -5\mu_1 & -3\mu_1 & 9\mu_1 & -\mu_1 & & & \\ & -5\mu_2 & -3\mu_2 & 9\mu_2 & -\mu_2 & & \\ & & \ddots & \ddots & \ddots & \ddots & \\ & & & -5\mu_{N-1} & -3\mu_{N-1} & 8\mu_{N-1} & \\ & & & & -5\mu_N & 5\mu_N & \end{pmatrix}. \tag{4.32}$$

The operators for a medium with a sharp boundary (Fig. 1b), or with a boundary between grids having different step sizes, can be obtained by defining modified operators for each region and then overlapping them as shown in Fig. 3(b). Note that there should be at least three nodes in each region, including boundary nodes. The first and last two rows of eq. (4.25) and the first two and last rows of eq. (4.28) should be used when there are only three nodes in a region.

5 NUMERICAL EXAMPLES

Except for Fig. 7, we use a single force point source with a Ricker wavelet source time function,

$$f(t)=\frac{\sqrt{\pi}}{2}\left\{\left[\frac{\pi(t-t_s)}{t_p}-\frac{1}{2}\right]^2\exp\left\{-\left[\frac{\pi(t-t_s)}{t_p}\right]^2\right\}\right\}, \tag{5.1}$$

where $t_p=40$ s is the peak period and $t_s=0$ s is the time shift of the peak. For the spherical *SH* case (Fig. 7), we use a double couple point source whose source time function is $f(t)=\delta(t)$. Causal Q is used throughout.

We define the 'spectrum error' as follows:

$$\text{spectrum error (per cent)}=\sqrt{\frac{\int|\delta\mathbf{c}|^2\,d\omega}{\int|\mathbf{c}^{(0)}|^2\,d\omega}}\times 100\ \text{(per cent)}. \tag{5.2}$$

The spectrum errors for the various cases considered in this section are listed in Table 1. We use analytic solutions for $\mathbf{c}^{(0)}$ whenever available. When no analytic solution is available, we use a numerical solution of the strong form of the equation of motion (e.g. Takeuchi & Saito 1972) with an extremely small step size. We then define the error of the numerical solution to be

$$\delta\mathbf{c}=\mathbf{c}-\mathbf{c}^{(0)}. \tag{5.3}$$

We consider *SH* waves at vertical incidence in a homogeneous medium with $\beta=5$ km s^{-1} and $Q=200$. The number of grid intervals is $N=100$ and $\Delta z=10$ km. We plot the error of the solutions obtained using the unmodified and modified operators (Fig. 5). The accuracy of the solutions obtained using the unmodified operators (eqs 3.5 and 3.8), which do not satisfy eq. (2.24), is very poor near the eigenfrequencies. In contrast, the modified operators $\mathbf{T}'$ and $\mathbf{H}'$ (eqs 3.31 and 3.33) approximately satisfy eq. (2.24) and thus suppress the degradation of the accuracy in the vicinity of the eigenfrequencies. The relative error using the modified operators is almost exactly equal to $k_z^2\Delta z^2/12$ (dashed line), as predicted in Section 3.3. Using the modified operators reduces the spectrum error by a factor of about 60 without changing the CPU time.

Next, we consider *SH* waves at vertical incidence in a two-layered medium with $\beta_1=5$ km s^{-1}, $\beta_2=10$ km s^{-1}, and $Q=200$. Fig. 6(a) gives results for a constant grid spacing ($\Delta z_1=\Delta z_2=10$ km s^{-1}), where $N_1=50$ and $N_2=50$. For Fig. 6(b) the number of elements per wavelength is constant for each layer: $\Delta z_1=10$ km, $\Delta z_2=20$ km, $N_1=50$ and $N_2=25$. Less CPU time was required for Fig. 6(b) than Fig. 6(a), but the modified operators were more accurate for the former.

We consider *SH* waves at vertical incidence in a medium with a velocity gradient. We use a constant $\mu=2.5\times10^{11}$ dyn cm^{-2} and a linear density gradient from $\rho=1$ g cm^{-3} at $z=0$ km to $\rho=0.25$ g cm^{-3} at $z=1000$ km. Thus the *S*-wave velocity changes smoothly from $\beta=5$ km s^{-1} at $z=0$ km to $\beta=10$ km s^{-1} at $z=1000$ km. We use $Q=200$, $\Delta z=10$ km and $N=100$. As there is no analytic solution, we use a solution obtained by numerical integration of the strong form of the equation of motion with an extremely fine grid as $\mathbf{c}^{(0)}$. The spectrum error for the modified operators is reduced by a factor of about 35.

We consider *SH* waves at vertical incidence in a homogeneous medium ($0\leq z\leq 1000$) with a radiation boundary condition at the bottom boundary ($z=1000$ km), $\beta=5$ km s^{-1}, $N=100$, and $Q=200$. The relative error for the unmodified and modified

Table 1. Spectrum errors.

Case	Figure	Spectrum Error	
		Unmodified	Modified
Homogeneous SH	5	62.7%	1.00%
Two Layer SH - Δz constant	6a	48.1%	1.47%
Two Layer SH - $k_{z\beta}\Delta z$ constant	6b	62.6%	1.02%
SH - Velocity gradient	-	39.3%	1.13%
SH - Radiation boundary	6c	11.1%	0.81%
P-SV Homogeneous	6d	32.1%	0.52%
P-SV Velocity gradient	-	21.1%	0.40%

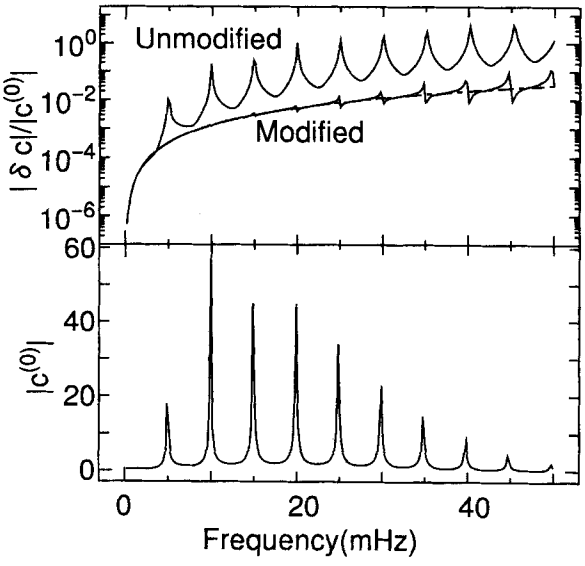

Figure 5. Comparison of the accuracy of solutions obtained using the modified and original operators for *SH* waves at vertical incidence in a homogeneous medium. We plot the relative error of both numerical solutions on a log scale (upper figure). We plot the amplitude of the analytic solution on a linear scale (lower figure). The predicted relative error for the modified operators, $k_z^2\Delta z^2/12$, is shown by the dashed line. Near the eigenfrequencies, the amplitude of the analytic solution, as expected, is largest. This is therefore the region where accuracy of the numerical solution is most important. As shown in the upper plot, the relative error of the unmodified operators is worst near the eigenfrequencies, but the modified operators suppress this degradation of accuracy.

operators is shown in Fig. 6(c). As there are no modes for this medium in the conventional sense, we do not see degradation of the accuracy near the eigenfrequencies. Nevertheless, the spectrum error of the modified operators is reduced by a factor of about 14.

Cummins *et al.* (1994a) derived modified operators for the *SH* (toroidal) problem in spherical coordinates. We compute synthetics (Fig. 7) for the isotropic part of the spherically symmetric earth model, PREM (Dziewonski & Anderson 1981). The source is a moment tensor point source at a depth of 600 km, and the source mechanism is $M_{r\theta} = M_{\theta r} = 1$ with all other components zero. The PREM Q model is used. A causal (Butterworth) filter was used for all the synthetics in Fig. 7. The first trace ('exact') is computed using the modified operators with an extremely fine grid ($N = 3200$) and is effectively exact. The second trace is the waveform computed using the modified operators ($N = 200$), and the fourth trace is the waveform computed using the unmodified operators ($N = 200$). The third trace ('residual') is the error (modified − exact) for the synthetic computed using the modified operators, and the fifth trace is the error of the synthetic for the unmodified operators.

We compute the 'waveform error' for the solutions obtained using the unmodified and modified operators as follows:

$$\text{waveform error (per cent)} = \sqrt{\frac{\int |u_{\text{num}} - u_{\text{exact}}|^2\, dt}{\int |u_{\text{exact}}|^2\, dt}} \times 100 \text{ (per cent)}. \tag{5.4}$$

As shown in Fig. 7, using the modified operators improves the waveform accuracy by a factor of about 30. The waveform error of 130 per cent for unmodified operators means that the amplitude of the residual is larger than the amplitude of the synthetic itself. The reason for this is the error of the phase of the synthetic for the unmodified operators. The arrows in Fig. 7 indicate the theoretical arrival times of the various body-wave phases. The body-wave arrivals are clearly visible in the 'exact' and 'modified' synthetics, but cannot be seen clearly in the 'unmodified' synthetics, due to the numerical error of the unmodified operators.

We consider a homogeneous medium with $\alpha = 5\sqrt{3}$ km s^{-1}, $\beta = 5$ km s^{-1}, $Q_\kappa = 10\,000$, and $Q_\mu = 100$, where κ is the bulk modulus. We use $\Delta z = 10$ km and $N = 100$. We compute solutions for an apparent velocity $c_x = 20$ km s^{-1}. The relative errors for the unmodified and modified operators are shown in Fig. 6(d). The dashed lines correspond to $k_\alpha^2\Delta z^2/12$ and $k_\beta^2\Delta z/12$, respectively. The relative error using the modified operators sometimes exceeds $k_\beta^2\Delta z^2/12$, perhaps because of the existence of the boundary error. The spectrum error for the modified operators is reduced by a factor of about 60.

In Fig. 8 we show the eigenfunction of the nearest mode (top), the operator error (second) and the solution errors for the unmodified and modified operators (third and bottom, respectively) at the frequency shown by the arrow in Fig. 6(d), which is in the vicinity of an eigenfrequency. As these quantities are complex, their absolute value is shown in Fig. 8. The operator error is

$$(\text{operator error})_{p\gamma} = \sum_{p'=0}^{N} \sum_{\gamma'=1}^{2} (\omega^2 \mathrm{T}_{p\gamma p'\gamma'} - \mathrm{H}_{p\gamma p'\gamma'}) \mathrm{c}^{(0)}_{p'\gamma'}, \tag{5.5}$$

where $\mathbf{c}^{(0)}$ is the analytic solution for a normal mode, and ω is the corresponding eigenfrequency. As the eigenfunction, operator error and solution error are complex, their absolute values are shown in Fig. 8. The solution error is

$$(\text{solution error})_{p'\gamma'} = \mathrm{c}_{p'\gamma'} - \mathrm{c}^{(0)}_{p'\gamma'}, \tag{5.6}$$

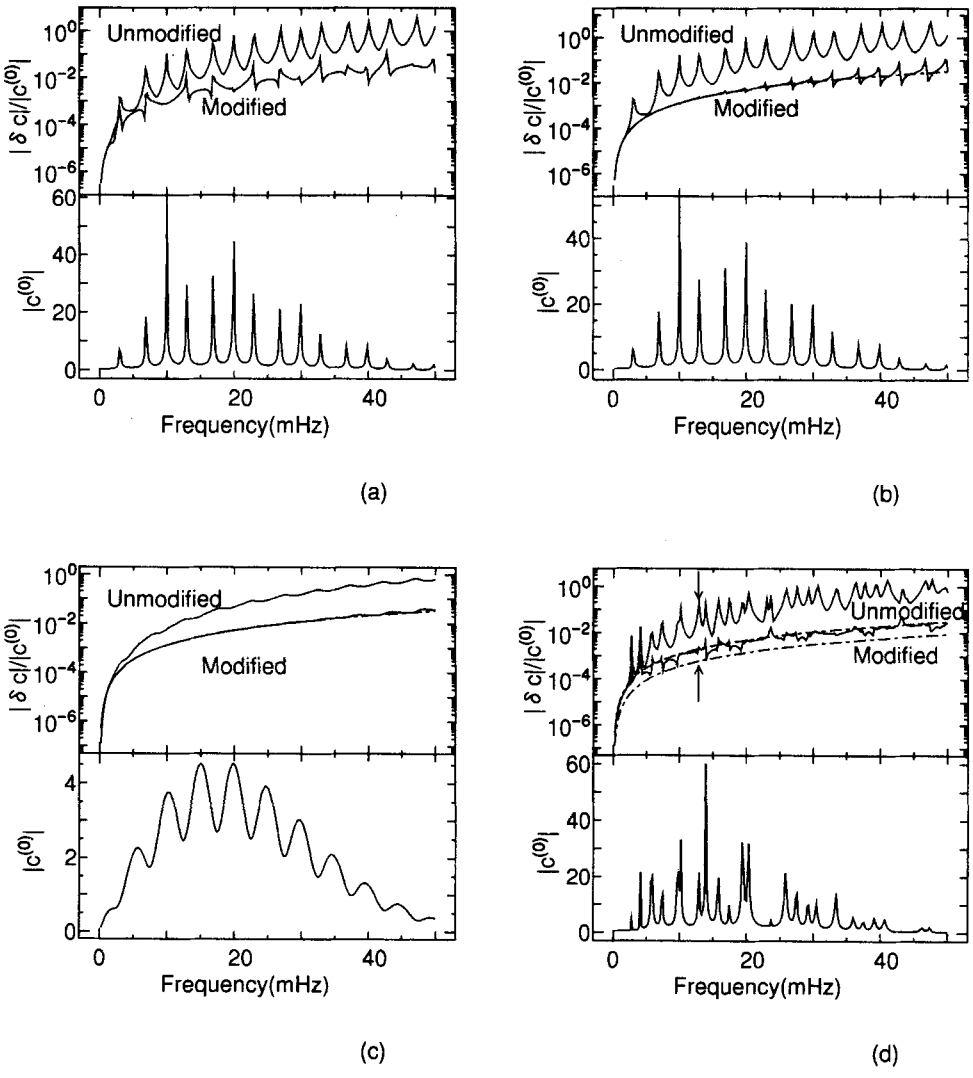

Figure 6. Relative error (upper half) and amplitude of the analytic solution (lower half). Other details are the same as in Fig. 5, except that the dashed line is omitted in Fig. 6(a), as $k_z\Delta z$ is not constant. (a) Results for the two-layered *SH* case with a constant grid interval ($\Delta z = 10$ km). (b) Results for the two-layered *SH* case with a constant number of elements per wavelength ($\Delta z = 10$ km in a slow segment, $\Delta z = 20$ km in fast segment). (c) Results for the homogeneous *SH* case with a radiation boundary condition. (d) Results for *P-SV* solutions for a homogeneous medium. Dashed lines correspond to $k_\alpha^2\Delta z^2/12$ and $k_\beta^2\Delta z^2/12$, where k_α and k_β are the z-components of the wavenumber vectors for *P* and *S* waves, respectively. The relative error using the modified operators sometimes exceeds $k_\beta^2\Delta z^2/12$, perhaps because of the existence of the boundary error.

where $\mathbf{c}$ is the numerical solution and $\mathbf{c}^{(0)}$ is the analytic solution. The solid lines show the error for the unmodified operators and the dashed lines show the error for the modified operators in the lower three plots.

As shown by the 'operator error' plots in Fig. 8, the unmodified operators have a non-zero basic error as well as a non-zero boundary error at the external boundary. The basic error of the modified operators is zero, but they have large boundary errors. As shown above in eq. (4.27), the net contribution of the boundary errors to $\mathbf{c}_m^*(\omega_m^2\boldsymbol{\delta}\mathbf{T} - \boldsymbol{\delta}\mathbf{H})\mathbf{c}_m$ is $O(\Delta z^2)$. However, as discussed in Section 2.1, the boundary error does not greatly affect the error of the solution; this is confirmed by the bottom figures in Fig. 8. The solution error for the modified operators is over 100 times smaller than the solution error for the unmodified operators, but both are essentially proportional to the eigenfunction. Thus Fig. 8 confirms that only that part of the operator error which is proportional to the eigenfunction is important.

Finally, we consider a medium with a smooth velocity gradient. We consider a constant $\rho = 1$ g cm^{-3} and $\lambda = 2.5 \times 10^{11}$ dyn cm^{-2}, and an inhomogeneous μ which varies linearly from $\mu = 2.5 \times 10^{11}$ dyn cm^{-2} at $z = 0$ km to $\mu = 5.0 \times 10^{11}$ dyn cm^{-2} at $z = 1000$ km. This means that the *P*- and *S*-wave velocities change smoothly from $\alpha = 5\sqrt{3}$ km s^{-1} and $\beta = 5$ km s^{-1} at $z = 0$ km to $\alpha = 5\sqrt{5}$ km s^{-1} and $\beta = 5\sqrt{2}$ km s^{-1} at $z = 1000$ km. We use $Q_\kappa = 10\,000$, $Q_\mu = 100$, $\Delta z = 10$ km and $N = 100$. We compute solutions for $c_x = 20$ km s^{-1}. The spectrum error (figure omitted) for the modified operators is about 50 times smaller than the spectrum error for the unmodified operators.

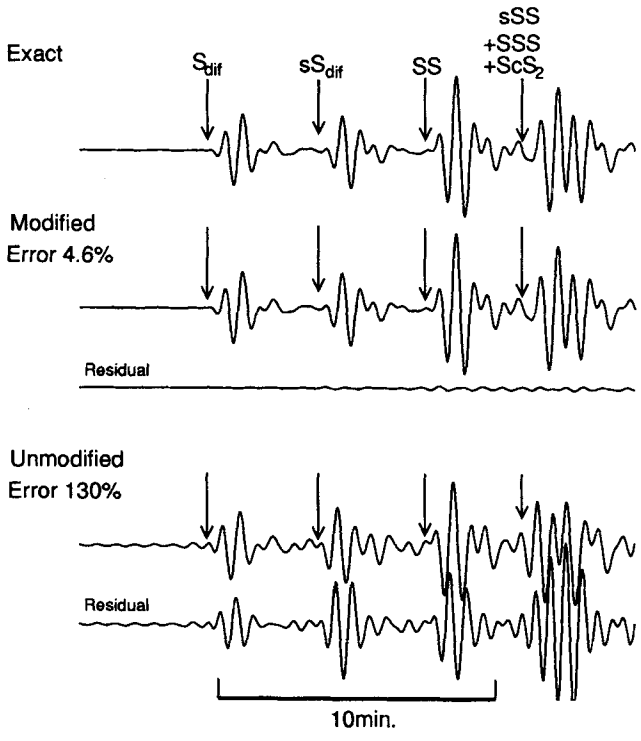

Figure 7. *SH* (toroidal) waveforms calculated for the laterally homogeneous spherical model PREM using the modified and the unmodified operators. The 'exact' solution was calculated using the modified operators for $N = 3200$ grid intervals. The 'modified' and 'unmodified' solutions were calculated using $N = 200$. The residuals are obtained by subtracting the exact synthetic from the 'modified' and 'unmodified' synthetics. The error is computed using eq. (5.4). Note that the error is worse than 100 per cent for the synthetics calculated using the unmodified operators because of the phase shift due to numerical dispersion.

6 DISCUSSION

As shown by the dashed lines in Figs 5 and 6(b)–(d), the relative error for the modified operators is a more or less predictable ($k_z^2 \Delta z^2/12$). The relation between the wavelength in the vertical direction, λ_z, and the vertical component of the wavenumber vector, k_z, is

$$\lambda_z = \frac{2\pi}{k_z}. \tag{6.1}$$

We thus have the following approximate relation between relative error and wavelength:

$$\text{relative error} = \frac{k_z^2 \Delta z^2}{12} = \frac{(2\pi)^2}{12} \frac{\Delta z^2}{\lambda_z^2} \approx \frac{3.3}{(\text{elements/wavelength})^2}. \tag{6.2}$$

We can obtain an estimate of the number of elements per vertical wavelength, $\lambda_z/\Delta z$, required to achieve a given relative error from eq. (6.2):

$$\text{elements/wavelength} = \frac{\lambda_z}{\Delta z} \approx \sqrt{\frac{3.3}{\text{relative error}}}. \tag{6.3}$$

Thus to achieve a relative error of $0.01 = 1$ per cent, we require about 18 elements/wavelength. Eq. (6.2) shows that if we use 8 elements/wavelength we obtain a relative error of about 5 per cent. This might be acceptable for forward modelling, but it is probably unacceptable for a formal inversion.

For a heterogeneous region, the relative error cannot be rigorously estimated. However, if we use a grid where the number of elements per wavelength is more or less constant, we can obtain acceptable estimates from eqs (6.2) and (6.3).

6.1 Future applications

It should be straightforward to extend the modified *P-SV* operators of the present paper to the laterally homogeneous spheroidal case considered by Cummins *et al.* (1994b) and the laterally heterogeneous case in spherical coordinates considered by Cummins *et al.* (1994c). It should also be straightforward to develop modified operators for a fluid medium along the same general lines of the *SH* operators in Section 3. Note that Geller & Ohminato (1994, Section 3) and Cummins *et al.* (1994b) show how to handle

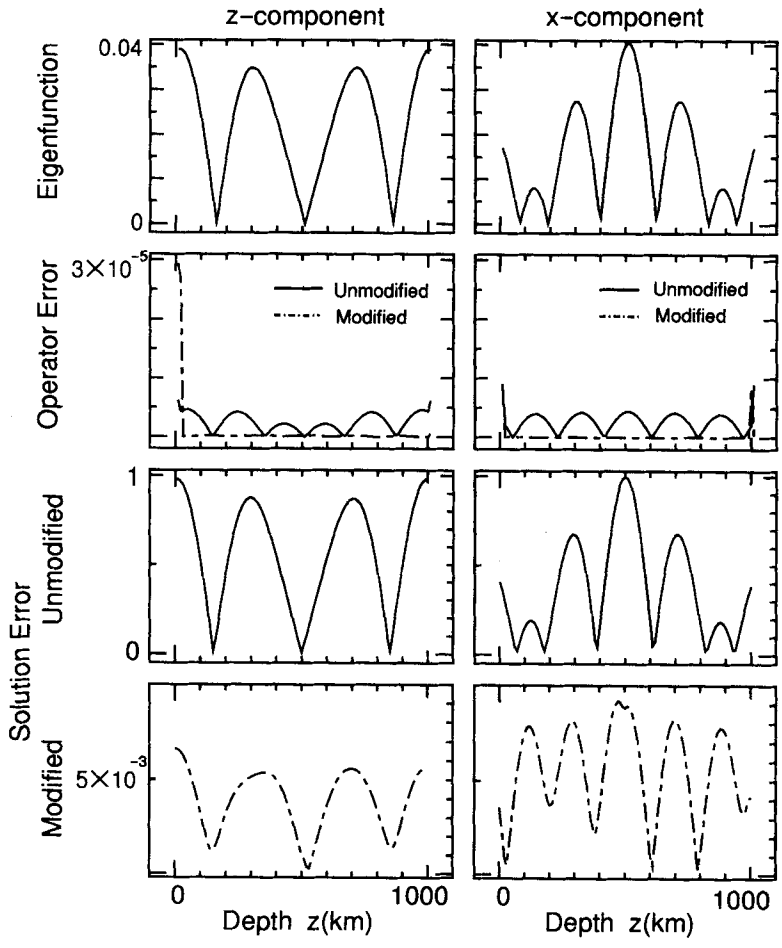

Figure 8. (Top) The absolute value of the eigenfunction whose eigenfrequency is indicated by the arrow in Fig. 6(d), (second) the operator error, and (bottom two rows) the solution error is for the unmodified and modified operators, respectively. The operator error and solution error are defined by eqs (5.5) and (5.6), respectively. The solid lines show the error for the unmodified operators, and the dashed lines show the error for the modified operators. We confirm that (1) if the operators have no basic error, the solution error will be very small; (2) regions that have large operator errors such as the external boundary do not necessarily have large solution errors. The amplitudes of the top, middle and lower two plots are not directly comparable, but the amplitude of the lowest two plots in each column are directly comparable. The eigenfunctions and operator errors were computed for a perfectly elastic medium, while the solution errors were computed for a medium with causal Q.

a mixed fluid–solid medium. Anisotropic media are not considered in this paper, but in principle there is no reason why our approach cannot also be applied to anisotropic media.

Our approach can also, in principle, be used in the time domain. Many finite-difference studies use a staggered grid, and treat velocity and stress as conjugate variables (e.g. Virieux 1986). We will report on modified operators for such approaches in a future work.

ACKNOWLEDGMENTS

This research was inspired by a study of the modified operators for the *SH* case by one of us (RG), G. Fujie and Y. Toda. We thank Phil Cummins and Tatsuhiko Hara for critically reading the manuscript. This research was partly supported by a grant from the Japanese Ministry of Education, Science and Culture (No. 06640542), and by the ISM Cooperative Research Program (ISM95·CRP-48). NT was supported by a JSPS Fellowship for Young Scientists.

REFERENCES

Cummins, P.R., Geller, R.J., Hatori, T. & Takeuchi, N., 1994a. DSM complete synthetic seismograms: SH, spherically symmetric, case, *Geophys. Res. Lett.*, **21**, 533–536.

Cummins, P.R., Geller, R.J. & Takeuchi, N., 1994b. DSM complete synthetic seismograms: P-SV, spherically symmetric, case, *Geophys. Res. Lett.*, **21**, 1663–1666.

Cummins, P.R., Geller, R.J. & Takeuchi, N., 1994c. Complete seismic wavefield calculations for strong upper mantle heterogeneity (abstract), *EOS, Trans. Am. geophys. Un.*, **75** (Fall Mtg Suppl.), 422.

Dziewonski, A.M. & Anderson, D.L., 1981. Preliminary reference Earth model, *Phys. Earth planet. Int.*, **25**, 297–356.

Geller, R.J. & Hara, T., 1993. Two efficient algorithms for iterative linearized inversion of seismic waveform data, *Geophys. J. Int.*, **115**, 699–710.

Geller, R.J. & Hatori, T., 1995. DSM synthetic seismograms using

analytic trial functions: plane-layered, isotropic, case, *Geophys. J. Int.*, **120,** 163–172.

Geller, R.J. & Ohminato, T., 1994. Computation of synthetic seismograms and their partial derivatives for heterogeneous media with arbitrary natural boundary conditions using the Direct Solution Method, *Geophys. J. Int.*, **116,** 421–446.

Geller, R.J., Hara, T., Tsuboi, S. & Ohminato, T., 1990. A new algorithm for waveform inversion using a laterally heterogeneous starting model (abstract in Japanese), *Seism. Soc. Jpn.*, Fall Meeting, 296.

Hara, T., Tsuboi, S. & Geller, R.J., 1991. Inversion for laterally heterogeneous earth structure using a laterally heterogeneous starting model: preliminary results, *Geophys. J. Int.*, **104,** 523–540.

Isaacson, E. & Keller, H.B., 1966. *Analysis of Numerical Methods,* Wiley, New York.

Korn, M., 1987. Computation of wavefields in vertically inhomogeneous media by a frequency domain finite-difference method and application to wave propagation in earth models with random velocity and density perturbations, *Geophys. J. R. astr. Soc.*, **88,** 345–377.

Lancaster, P., 1966. *Lambda-matrices and Vibrating Systems,* Pergamon, Oxford.

Liu, H., Anderson, D.L. & Kanamori, H., 1976. Velocity dispersion due to anelasticity; implications for seismology and mantle composition, *Geophys. J. R. astr. Soc.*, **47,** 41–58.

Marfurt, K.J., 1984. Accuracy of finite-difference and finite-element modeling of the scalar and elastic wave equations, *Geophysics,* **49,** 533–549.

Nolet, G., Grand, S.P. & Kennett, B.L.N., 1994. Seismic heterogeneity in the upper mantle, *J. geophys. Res.*, **99,** 23 753–23 766.

Park, J. & Gilbert, F., 1986. Coupled free oscillations of an aspherical, dissipative, rotating earth: galerkin theory, *J. geophys. Res.*, **91,** 7241–7260.

Strang, G. & Fix, G.J., 1973. *An Analysis of the Finite Element Method,* Prentice-Hall, Englewood Cliffs, NJ.

Takeuchi, H. & Saito, M., 1972. Seismic surface waves, *Meth. Comput. Phys.*, **11,** 217–295.

Tarantola, A., 1984. Inversion of seismic reflection data in the acoustic approximation, *Geophysics,* **49,** 1259–1266.

Virieux, J., 1986. P-SV wave propagation in heterogeneous media: Velocity-stress finite-difference method, *Geophysics,* **51,** 889–901.